

# Solar Assisted Power Generation (SAPG): Investigation of Solar Preheating of Feedwater

BY  
Warrick Tait Pierce



*Assignment presented in partial fulfilment of the requirements for the degree of  
Master of Engineering (Mechanical) in the Faculty of  
Engineering at Stellenbosch University*

Supervisor: Paul Gauché

March, 2013

## Declaration

By submitting this assignment electronically, I declare that the entirety of the work contained therein is my own, original work, that I am the sole author thereof (save to the extent explicitly otherwise stated), that reproduction and publication thereof by Stellenbosch University will not infringe any third party rights and that I have not previously in its entirety or in part submitted it for obtaining any qualification.

March 2013

Copyright © 2013 Stellenbosch University

All rights reserved

## Abstract

Solar Assisted Power Generation (SAPG) can be seen as a synergy of solar and fossil plants – combining the environmental benefits of the former and the scale, efficiency and reliability of the latter. SAPG offers great potential for cost effective utilization of solar energy on utility scale and could accelerate the adoption of solar thermal energy technologies in the short and medium term, especially in countries with a significant coal base and a good solar resource such as Australia, China, United States, India and South Africa.

SAPG is the replacement of bled-off steam in a Regenerative Rankine power cycle. Power plant simulations were performed using weather data for Lephalale, South Africa (Matimba power station). With an increase in the solar field outlet temperature, an increase in overall solar to electric efficiency was observed, superior to a stand-alone Solar Thermal Power Plant(s) (STPP) at similar temperatures.

The performance of four solar collector technologies was compared: flat plate, evacuated tube, Linear Fresnel (LF) and Parabolic Trough (PT). This comparison was limited to the normal incidence angles of irradiation. For this application, non-concentrating technologies are not competitive.

For non-normal incidence angles, annual simulations were limited to PT and LF at final feedwater heater temperatures. The actual aperture area of around 80 000 m<sup>2</sup> was used (50 MW thermal based on LF). On an equal aperture area basis, PT outperforms LF significantly. For the conventional North-South arrangement, LF needs to be around 53% of the specific installation cost (in \$/m<sup>2</sup> aperture area) of PT to be cost competitive

A SAPG plant at Lephalale was compared to a stand-alone Solar Thermal Power Plant STPP in a good solar resource area, namely Upington, South Africa – Parabolic Trough solar collector fields of equal size were considered for both configurations. It was found that the annual electricity generated with a SAPG plant is more than 25% greater than a stand-alone STPP. If the cost of SAPG is taken as 72% of the cost of a stand-alone STPP, this translates into SAPG being 1.8 times more cost effective than stand-alone STPP. Furthermore, SAPG performs better in high electricity demand months (South African winter – May to August).

Stand-alone STPP have been adopted in South Africa and are currently being built. This was achieved by the government creating an attractive environment for Independent Power Producers (IPP). Eskom, the national power supplier, is currently investigating solar boosting at existing Eskom sites. This report argues that on a national level, SAPG, specifically solar preheating of feedwater, is a more viable solution for South Africa, with both its significant coal base and good solar resource.

## Opsomming

Son ondersteunde krag generasie (SOKG) kan gesien word as sinergie van sonkrag en fossiele brandstof aanlegte – dit voeg die omgewings voordele van die eersgenoemde en die grote, effektiwiteit en betroubaarheid van die laasgenoemde by mekaar. SOKG opper groot potensiaal vir koste effektiewe gebruik van son energie op nutsmaatskappyskaal en kan die aanvaarding van sontermiese energietechnologieë in die kort en medium termyn versnel, veral in lande met beduidende kool reserves en goeie sonkrag voorkoms soos Australië, China, Verenigde State van Amerika, Indië en Suid-Afrika.

SOKG impliseer die vervanging van aftap stoom in die regeneratiewe Rankine krag kringloop. Kragstasie simulaties was gedoen met die gebruik van weer data van Lephalale, Suid-Afrika (Matimba kragstasie). Met die toename van die sonveld uitlaat temperatuur kon oorhoofse son-na-elektrisiteit effektiwiteit vasgestel word, wat hoër is as die van alleenstaande sontermiese krag stasie (STKS) by soortgelyke temperature.

Die effektiwiteit van vier son kollekteerder tegnologieë was vergelyk: plat plaat, vakuum buis, lineêre Fresnel (LF) en paraboliese trog (PT). Die vergelyking was beperk tot normale inval van bestraling. Vir hierdie toepassing is nie-konsentreerende tegnologie nie mededingend nie.

Vir nie-normale inval hoeke was jaarlange simulaties beperk tot PT en LF by finale voedingswater temperatuur. Die werklike opening area van omtrent 80 000 m<sup>2</sup> was gebruik (50 MW termies gebaseer op LF). By gelyke opening area, uitpresteer PT LF beduidend. Vir die gebruiklike Noord-Suid rangskikking benodig LF omtrent 53% van die spesifieke installasie kostes (in \$/m<sup>2</sup> opening area) van PT om kostes mededingend te kan wees.

‘n SOKG aanleg by Lephalale was vergelyk met alleenstaande STKS in die goeie son voorkoms gebied van Upington, Suid-Afrika – Paraboliese trog kollekteerder velde van gelyke grote was oorweeg vir al twee konfigurasies. Dit was gevind dat die jaarlikse elektrisiteit gegenereer vanaf SOKG meer as 25% is as die van alleenstaande STKS. Indien SOKG oorweeg word met 72% van die kostes van alleenstaande STKS, dan beteken dit dat SOKG 1.8 keer meer koste effektief is as alleenstaande STKS. Verder, SOKG presteer beter in die hoer elektrisiteitsnavraag maande (Suid-Afrikaanse winter – May tot Augustus).

Alleenstaande STKS is gekies vir Suid-Afrika en word tans gebou. Dit is bereik deur dat die regering ‘n aantreklike omgewing geskep het vir onafhanklike krag produsente. Eskom ondersoek tans SOKG by bestaande Eskom persele. Hierdie verslag beweer dat op nasionale/Eskom vlak, SOKG, besonders son voorverhitting van voedingswater, meer haalbare oplossing is vir Suid-Afrika met sy beduidende koolreserwes en goeie son voorkoms.

## Acknowledgements

*Holy, holy, holy is the LORD of hosts:  
The whole earth is full of his glory (Isaiah 6:3)*

*In that day every place where there used to be a thousand vines, worth a thousand shekels of silver, will become briars and thorns (Isaiah 7:23)*

*Learn to do good; seek justice, correct oppression; bring justice to the fatherless,  
plead the widow's cause (Isaiah 1:17)*

Let us become a generation that stands up for justice, a generation that diligently fights oppression.

This project would not be possible without the generosity of the John Thompson Boilers company (JTB). They funded the studies and allocated a portion of my working hours to this research. For this, I would like to specifically thank my boss, Quintus Engelbrecht. The practical support of JTB was much appreciated – our Divisional Chief Executive Officer, Andy Abbey, even requested power plant data from Eskom on my behalf.

Dr Richter, a visiting academic from the German Aerospace Center DLR, took the time to listen to research findings and made the effort to provide feedback, even contacting world experts in the field. Thank you for valuable input.

Professor Harms translated my abstract to an *opsomming*. Thank you for your assistance at very short notice.

James Joubert provided a ‘skeleton’ for Visual Basic coding which realized the annual hourly simulations. Thank you for saving me precious time. Cobus Burger kindly offered to review the document in its entirety. Thank you for your work in the ‘graveyard shift’.

Lastly, I would like to thank Paul Gauché for accepting me and my topic at late notice. His guidance towards the bigger picture is greatly valued. STERG now has a research starting platform in the very relevant field of solar assisted power generation.

## Table of Contents

Declaration.....	i
Abstract.....	ii
Opsomming.....	iii
Acknowledgements.....	iv
List of Tables.....	vii
List of Figures.....	viii
Nomenclature.....	x
1. Introduction .....	1
1.1 Motivation.....	2
1.2 Research objectives.....	3
1.3 Project outline .....	3
2. Literature review .....	4
2.1 Power cycles .....	4
2.1.1 Carnot cycle.....	4
2.1.2 Rankine cycle.....	5
2.1.3 Reheat Rankine cycle.....	7
2.1.4 Regenerative Rankine cycle.....	8
2.2 Solar Assisted Power Generation (SAPG).....	9
3. Steady State Thermal Power Plant Model.....	10
3.1 Modelling.....	11
3.1.1 Software tool.....	11
3.1.2 Components .....	11
3.1.3 Description.....	11
3.2 Model validation.....	16
4. Solar Assisted Power Generation (SAPG) Model.....	18
4.1 Solar field.....	19
4.1.1 Software tool.....	19
4.1.2 Solar field integration.....	19
4.1.3 Solar collector technologies .....	20
4.2 Modelling.....	21
4.2.1 Description.....	21

4.2.2	Scenarios .....	24
4.3	Model validation .....	30
5.	Results.....	31
5.1	Steady state thermal power plant model (regenerative measures).....	31
5.2	SAPG .....	33
5.2.1	Various SF .....	33
5.2.2	Various solar collectors .....	33
5.2.3	SAPG vs. stand-alone STPP.....	38
6.	Conclusions .....	40
7.	Recommendations.....	41
	List of References.....	42

## List of Tables

Table 1: Steady state thermal power plant model inputs – scenario selection .....	12
Table 2: Steady state thermal power plant model inputs - state specifications.....	12
Table 3: Steady state thermal power plant model inputs - efficiencies.....	12
Table 4: Temperature ranges and investigated solar collectors .....	20
Table 5: SAPG model inputs – scenario selection .....	22
Table 6: SAPG model inputs - state specifications .....	22
Table 7: SAPG model inputs - efficiencies .....	22
Table 8: Summary of solar collector performance (Kalogirou, 2003).....	25
Table 9: Summary of weather conditions for investigated sites (Meteonorm, 2010) .....	28
Table 10: Parabolic trough cost assessment (NREL, 2010), exchange rate used 1 USD = 9 ZAR (presented in thousands) .....	29
Table 11: Comparison of outputs from literature and developed model.....	30



## List of Figures

Figure 1: Heat engine layout.....	4
Figure 2: T-s diagram of Carnot cycle .....	5
Figure 3: T-s diagram of the ideal (left) and Rankine cycle including isentropic efficiency for a pump and turbine .....	6
Figure 4: T-s diagram displaying isentropic efficiency for pump (exploded view (t – theoretical and r – real/actual)).....	6
Figure 5: Schematic (left) and T-s diagram of practical Rankine cycle (Cengel 2002).....	7
Figure 6: Schematic of a 200 MWel power plant (Yan <i>et al.</i> , 2010).....	10
Figure 7: Graphical description of ratio of heating .....	13
Figure 8: Schematic diagram of heat and mass balances of a generic power plant.....	14
Figure 9: Water/steam property labels in (a) typical (b) extraction steam, and the units thereof (c) .....	14
Figure 10: Improvement in thermal efficiency with feed water heating (no reheating (data points (blue markers) are referenced from Sherry, 1971)).....	17
Figure 11: Reheat regenerative cycle, in a 600 MW subcritical fossil power plant (Singer, 1991).....	18
Figure 12: Direct integration of the solar field .....	19
Figure 13: SAPG model representation (comparison to Figure 11 possible (solar off))...	23
Figure 14: SAPG opposing 'forces' .....	24
Figure 15: Solar thermal collector efficiency ( $G = 590 \text{ W/m}^2$ ).....	26
Figure 16: Relative size of the solar field to the Matimba power station .....	27
Figure 17: Map of Southern Africa indicating the stand-alone STPP site (Upington) and the SAPG site (Lephalale) (Google Earth) .....	28
Figure 18: Cost breakdown of a Parabolic Trough power plant.....	29
Figure 19: Efficiency improvements with preheating of boiler feedwater .....	32
Figure 20: Effect of regenerative heating.....	32
Figure 21: Annual total efficiencies for various solar field integrations.....	34

Figure 22: Performance per cost comparison for various solar collectors (relative to LF at SF6) .....	34
Figure 23: Performance comparison of parabolic trough and linear Fresnel (SF 6) .....	35
Figure 24: (a) Simulated incidence angle modifiers for Parabolic Trough and Linear Fresnel (b) definitions used: $\theta_t$ is transversal IAM and $\theta_l$ is longitudinal IAM (Morin <i>et al.</i> , 2011) .....	36
Figure 25: Average national electricity demand for South Africa (Eskom, 2009) .....	36
Figure 26: Solar thermal output from SF - clear summer day (20 December) .....	37
Figure 27: Solar thermal output from SF - clear winter day (19 June) .....	37
Figure 28: Energy breakdown of annual totals for stand-alone STPP and SAPG .....	39
Figure 29: Comparison of electricity generated for stand-alone STPP and SAPG .....	39

## Nomenclature

### Latin Symbols

$G$	solar radiation
$h$	specific enthalpy
$H$	total enthalpy
$\dot{m}$	mass flow rate
$P$	pressure
$Q$	heat
$s$	specific entropy
$T$	temperature
$x$	steam quality

### Greek Symbols

$\Delta$	difference
$\theta$	solar angle
$\eta$	efficiency

### Subscripts

$amb$	ambient
$db$	dry bulb
$el$	electric
$H$	high temperature level
$i$	longitudinal
$L$	low temperature level
$sat$	saturated
$t$	transversal
$th$	thermal

## Abbreviations

CSP	Concentrated Solar thermal Power
DNI	Direct Normal Irradiation
DSG	Direct Steam Generation
EPC	Engineer Procure Construct
ET	Evacuated Tube
E-W	East-West
FP	Flat Plate
FWH	Feedwater Heater
GCV	Gross Caloric Value
GHG	Greenhouse Gases
GHI	Global Horizontal Irradiation
HMB	Heat and Mass Balance
HP	High Pressure
IAPWS	International Association for the Properties of Water and Steam
IAM	Incidence Angle Modifier
IEA	International Energy Agency
IP	Intermediate Pressure
IPP	Independent Power Producers
LF	Linear Fresnel
LP	Low Pressure
LTI	Latitude Tilt Irradiation
NREL	National Renewable Energy Laboratory
N-S	North-South
PT	Parabolic Trough
REIPPP	Renewable Energy Independent Power Producers Programme
RH	Reheater
SAM	System Advisor Model
SAPG	Solar Assisted Power Generation
SF	Solar Field
SH	Superheater
SM	Solar Multiple
STPP	Solar Thermal Power Plants
TES	Thermal Energy Storage

## 1. Introduction

The world's energy demands are increasing exponentially. These needs have been met with fossil fuel derivatives in recent times. Although conflicting estimates of fossil fuel reserves have been made, the fact remains that these reserves are depleting. This and the increase in energy demands will lead to energy requirements not being met. The current energy generation setup is unsustainable.

More than 80% of the world's primary energy supply is from fossil fuels (IEA, 2012). This dependence is even greater in South Africa where more than 90% of electricity generation capacity is coal fuelled (Eskom, 2012). Fossil fuels have and continue to provide a cheap and reliable energy source. Recent research has highlighted that these benefits come at a cost, for instance the release of Greenhouse Gases (GHG) into the atmosphere - a contributing factor to climate change.

The harnessing of renewable energy (RE) resources has been identified as a sustainable energy alternative. However, the relatively low energy intensity, technology immaturity and/or intermittency of RE forms make these alternatives costly. There is an on-going pursuit to reduce the costs of RE technologies through improved technological developments and mass production. This in conjunction with increasing 'conventional' energy costs are making RE technologies more attractive.

Solar energy technologies (abbreviated to simply 'solar' hereafter) specifically have gained much attention as a viable solution for large scale power generation. With solar, as with other RE forms, intermittency of supply needs to be addressed. A viable solution to address dispatchability is the integration of solar thermal plants into conventional fossil plants – Solar Assisted Power Generation (SAPG)<sup>1</sup> can be seen as a synergy of solar and fossil plants, combining the environmental benefits of the former and the scale, efficiency and reliability of the latter. SAPG offers great potential for cost effective utilization of solar energy on a utility scale and could accelerate the adoption of solar thermal energy technologies in the short and medium term, especially in countries with a significant coal base and good solar resource such as Australia, China, United States, India and South Africa. It is therefore not surprising that the national power supplier Eskom has shown interest in this technology.

---

<sup>1</sup> Other terms such as solar boosting, solar augmentation and solar aided are commonly used

## 1.1 Motivation

The three pillars to a more environmentally friendly energy solution are: energy efficiency, renewable energy technologies and cleaner technologies. In general, energy needs to be both used more wisely and the generation thereof needs to be substituted with renewable energy sources. This substitution is a prerequisite for sustainable development.

There are various ways of integrating solar thermal energy into fossil power plants, for instance:

- solar production of main steam (high pressure steam)
- solar production of intermediate steam
- solar preheating of feedwater

The latter is the most effective means (Petrov *et al.*, 2012, Siros *et al.*, 2012). This is not surprising as solar preheating of feedwater is achieved at lower temperature ranges than main and intermediate steam production. Only solar preheating of feedwater is considered in this work and is referred to as SAPG throughout the text.

SAPG is the replacement of bled-off steam in a Regenerative Rankine power cycle. The bled-off steam is extracted from the steam turbine. This is used to preheat the boiler's feedwater. The overall cycle efficiency is increased at the cost of reduced steam flow through the steam turbine and thus lower work output is achieved. SAPG preheats feedwater with solar thermal energy, thereby supplementing turbine extracted steam and thus work output can be increased (boosting mode) or fuel consumption can be reduced (fuel saver mode).

Numerous authors have shown with energy and exergy analysis that solar thermal energy is more effectively employed in SAPG than in stand-alone Solar Thermal Power Plants (STPP) (Petrov *et al.*, 2012, Yang *et al.*, 2011, Gupta & Kaushik, 2010). Some of the other advantages of this synergy are given by Hu *et al.*, (2010):

- SAPG can be integrated into existing power stations and therefore at a relatively low implementation cost. The same environmental and social benefits are achieved as with stand-alone STPP
- SAPG is run in parallel to conventional power plants with minimal risk of operation disturbances
- Conventional power plants provide storage components to address intermittency of solar energy
- SAPG can be implemented in a modular manner
- Feedwater preheating has various heating requirements in terms of quantity and quality. The latter allows for low temperature solar collectors to be implemented.

## 1.2 Research objectives

This report aims to investigate SAPG in terms of feedwater heating. Similar efforts have been performed by Yan *et al.* (2010). However, certain constraints and complexities of power plant modelling were not included and not within the South African context. This study aims to:

- enhance the level of power plant modelling, specifically boiler limitations, variable condenser pressure and solar field complexities
- consider various solar collectors
- perform hourly annual simulations
- consider the South African solar resource
- compare SAPG to stand-alone STPP

Following a generic steady state thermal power plant model, a case study of the integration of flat plate, evacuated tube, Linear Fresnel and Parabolic Trough solar collectors into a power station (600 MW electric) will be used to portray the potential capabilities of SAPG.

## 1.3 Project outline

This section presents the basic layout of this project and provides a short description for each chapter. This report is divided into three main sections.

### **Section A: Introduction**

In Chapter 1, a brief introduction to the field of renewable energy, specifically SAPG is given. The research objectives and the project outline are described. A literature review is presented in Chapter 2 to provide a basis for this project.

### **Section B: Modelling**

Modelling of SAPG is investigated beginning with a basic Rankine cycle. The chapter is concluded with a SAPG model.

### **Section C: Data Presentation and Discussion**

This section presents the results, conclusions and recommendations that stem from the work done.

## 2. Literature review

Firstly, basic modelling of a conventional fossil fired power plant based on a Rankine cycle is presented. Recent studies of SAPG conclude this section.

### 2.1 Power cycles

Steam is the most common working fluid used in vapour power cycles. The preference of steam is due to its attractive properties such as abundance (high availability), affordability and good heat transfer characteristics, for instance high enthalpy of evaporation and high specific heat. A steam power plant is an example of a heat engine with water and steam as working fluid. Heat  $Q_H$  ( $Q_{in}$ ) is added to working fluid in a boiler and heat  $Q_L$  ( $Q_{out}$ ) is rejected from working fluid in a condenser, Figure 1. Work is achieved as working fluid the cycle.

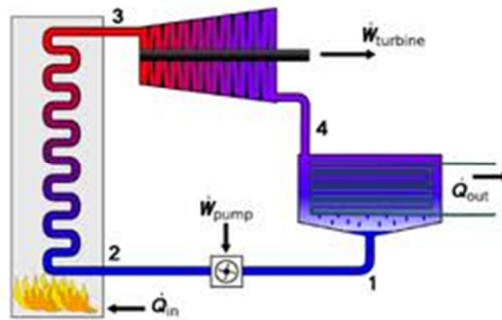


Figure 1: Heat engine layout

#### 2.1.1 Carnot cycle

The most efficient cycle operating between two temperature levels is the Carnot cycle. This is the ideal case. It considers heat input (process 2-3 in Figure 1) and rejection (process 4-1) as reversible and isothermal, and compression (process 1-2) and expansion (process 3-4) as isentropic (constant entropy). Figure 2 shows a T-s diagram of a Carnot cycle. The efficiency of such a system is dependent on the temperatures of heat source and sink, Eq. 1. For instance, consider a boiler operating at 300°C (573K) saturated steam and a heat sink of 50°C (323K). This equates to a Carnot efficiency of 0.44.

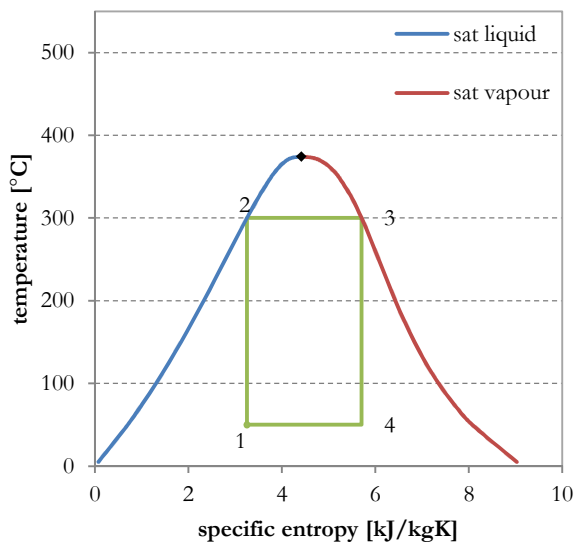
Some of the realities that are not included in the Carnot cycle are: within process 3-4, the steam turbine will need to handle ‘wet’ steam with low quality. The liquid droplets can be a source of serious erosion of blades. Steam quality  $x$  of above around 90% is typically required. For the compression process 1-2, a compressor needs to handle two phases. This is not practical. In short, the Carnot cycle should be seen as the upper limit and actual efficiencies are significantly lower.



### 2.1.2 Rankine cycle

The impracticalities of the Carnot cycle can be addressed by superheating the steam in the boiler, therefore point 3 moves from the saturated vapour line into the superheated vapour region, as shown in Figure 3. Furthermore, process 4-1 is condensed to the saturated liquid line. The former addresses steam quality and the latter allows pumping of liquid only, which is significantly less energy intensive than pumping a liquid vapour mixture.

The mentioned cycle is ideal as irreversibilities within individual components and connecting piping are omitted. For instance, fluid friction and heat losses are two common sources of irreversibilities. Therefore, pumps (typically the feedwater pumps of the boiler) need to raise the liquid pressure sufficiently above the ideal cycle pressure. Furthermore, the temperature after the boiler needs to be sufficiently higher than the ideal cycle temperature. To cater for irreversibilities within the pump and turbine, isentropic efficiencies are included, typically around 85% for both. The effects of these efficiencies are displayed in Figure 3 (right). As liquid water is near incompressible, the effect of pump isentropic efficiency on the T-s diagram is not noticeable. An exploded view of T-s diagram displays this effect in Figure 4.



$$\eta_{Carnot} = 1 - \frac{T_{1,4}}{T_{2,3}} \quad (1)$$

T in Kelvin

Figure 2: T-s diagram of Carnot cycle

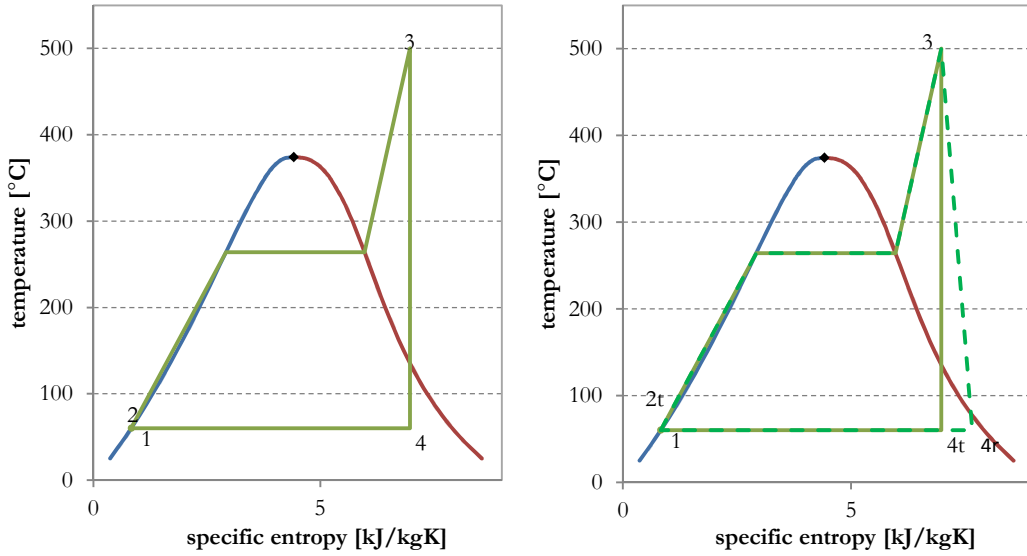


Figure 3: T-s diagram of the ideal (left) and Rankine cycle including isentropic efficiency for a pump and turbine

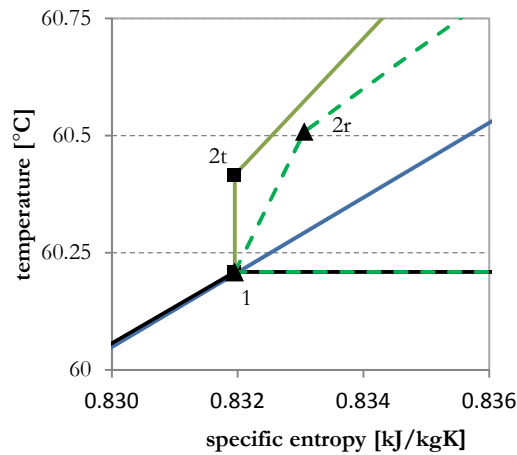


Figure 4: T-s diagram displaying isentropic efficiency for pump (exploded view (t – theoretical and r – real/actual))

An example of a practical Rankine cycle is presented in Figure 5. The Carnot, ideal and practical Rankine thermal cycle efficiencies for the example are 64.5, 43.6 and 36.1% respectively. It should be noted that the thermal efficiency of the boiler is not included; therefore the conversion of fuel to thermal energy is omitted. For utility boilers firing coal this is typically above 85% based on Gross Caloric Value (GCV) of fuel.

To improve the efficiency of the Rankine cycle a basic principle exists, namely to increase the average temperature at which heat is transferred to the working fluid and decrease the average temperature at which heat is rejected from the working fluid. This is realized by means of:

- increasing boiler output temperature
- decreasing condenser pressure
- increasing boiler pressure

There are practical limitations to achieving these. Material limitations to increasing boiler temperature and pressure are examples of such constraints. With elevated temperatures superheaters need to incorporate more ‘exotic’ and therefore more expensive materials. For the condenser pressure, atmospheric conditions and availability of cooling media are limitations. To this extent, and as a power plant consists of various components, it needs to be optimised as an integrated system reducing the practical limitations, still keeping costs as the ultimate consideration.

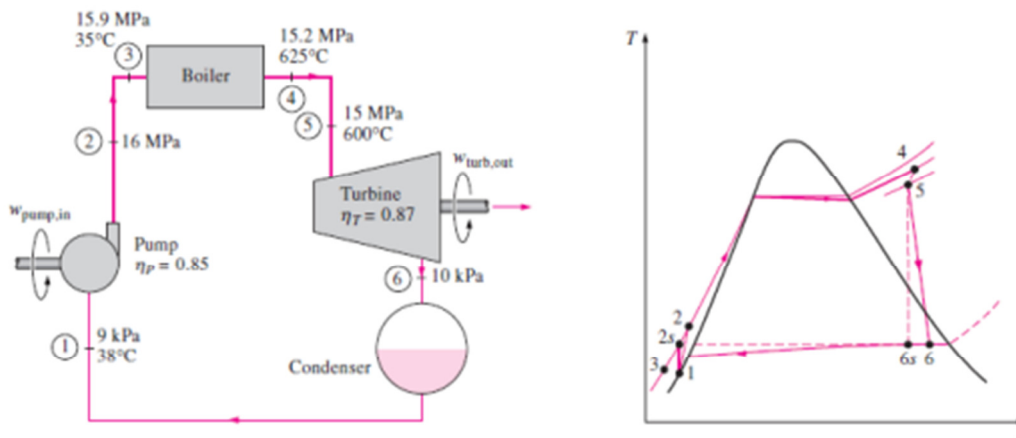


Figure 5: Schematic (left) and T-s diagram of practical Rankine cycle (Cengel 2002)

### 2.1.3 Reheat Rankine cycle

It was stated in a previous section that a means to increase the overall power plant efficiency is to raise the boiler operating pressure. This would require higher capacity feedwater pumps. Additionally the cost of water treatment increases substantially with pressure. To raise the boiler pressure is achievable and is currently employed. However, due to the increased pressure before the steam turbine, unacceptable moisture content in steam may be encountered in the final stages of the turbine. For instance, if the turbine input pressure is raised from 30 to 150 (bar)<sup>2</sup> and in both cases the steam is superheated to 600°C, and assuming isentropic expansion, the moisture content of steam is increased from 8.6% to 19.6%. As mentioned, liquid droplets can be a source of serious erosion of turbine blades and possibly result in equipment failure.

<sup>2</sup> If not indicated otherwise then pressure is given as absolute

To increase the temperature of superheated steam accordingly with increasing pressure would resolve the steam quality issue. For instance, for the example given to keep steam quality constant the temperature would need to be increased from 600°C to 938°C. This is problematic due to metallurgical limitations.

The industry solution is reheating. Steam is partially expanded in high pressure stages of the turbine then intermediate pressure steam is reheated in the boiler and then expanded in lower pressure stages (Figure 6). Reheat temperature is similar to inlet temperature of first stages. With reheating, the average temperature at which heat is added is increased and thus efficiency is increased. It should be noted that this same efficiency improvement could be achieved by simply raising the turbine inlet temperature.

Reheating is commonly implemented in utility sized power plants. The optimum reheat pressure is around  $\frac{1}{4}$  of high pressure (HP) turbine inlet pressure but can vary from 0.2 to 0.4 (Cengel & Boles, 2002, Habib *et al.*, 1999). The increase in efficiency is around 5% for first stage and approximately half for subsequent stage(s). Double reheat is used only for super-critical (above 221 bar) power plants (Cengel & Boles, 2002).

#### 2.1.4 Regenerative Rankine cycle

Previous sections discussed efficiency improvements by means of increasing temperature and pressure of superheated steam inputs to the steam turbine. The Regenerative Rankine cycle increases the average temperature at which heat is added by increasing the boiler input temperature. This is achieved with feedwater preheating. Steam is extracted from the turbine and used to heat feedwater. This reduces the amount of work generated by the turbine as steam is redirected from expanding further. This sacrifice is for the increased efficiency of the overall power cycle. Additionally, regeneration allows for deaeration of the feedwater and reduces the large volume flow rate (due to relative low densities) of the final stages of the turbine. Regeneration is used in all modern power plants.

The feedwater preheating with extracted steam from the turbine is achieved with direct (open) or closed feedwater heater (FWH). A direct FWH is a mixing chamber where feedwater and extracted steam come into direct contact. This promotes favourable heat transfer characteristics and is simple and affordable. The two streams need to be at the same pressure and one pump is required per direct FWH. A deaerator is an example of a direct (open) FWH.

With closed FWHs the two streams are separate and therefore do not need to be at the same pressure and thus do not require additional pumps. However, mixing is less intimate and therefore less effective and the heater is more complex and costly. Modern power plants employ combinations of direct and closed FWH.

## 2.2 Solar Assisted Power Generation (SAPG)

Solar Assisted Power Generation (SAPG) is the replacement of bled-off steam in a Regenerative Rankine power cycle with solar augmentation. SAPG, specifically through feedwater heating, preheats the feedwater with solar thermal energy and thus work output can be increased or fuel consumption can be reduced.

The overall efficiency of a power plant is dependent on, *inter alia*, the temperature of the heat source – efficiency improves with increasing temperature. For this reason few attempts have been made to employ low or medium solar heat for power generation. With SAPG, the heat source temperature is not limited by the solar input temperature. Thus, SAPG is an effective way to utilise low or medium solar heat for power generation (Yang *et al.*, 2011).

Despite the apparent gains to be had countries, with the exception of Australia, have been conservative in adopting projects in the field of solar preheating of feedwater.

The Liddell solar boost venture in North-South Wales (NSW), Australia by Novatec is one the first large scale commercial projects of the integration of a solar thermal technology with a conventional power plant (Novatec Solar, 2012). Direct Steam Generation (DSG) Linear Fresnel solar technology is employed and incorporated into the HP feedwater preheater. Within a year the complete project was built and integrated into a conventional 2 000 MW electric coal fired power plant and has been operational since March 2012 (Paul *et al.*, 2012).

The Cogan Creek solar boost project in Queensland, Australia by CS Energy will be the largest SAPG in the world – a 44 MW thermal Compact Linear Fresnel (CLF) solar technology solution provided by Areva (Kogan Creek Solar Boost Project, 2012).

SAPG projects in the field of solar preheating of feedwater are being realised on a large scale. SAPG is especially relevant to South Africa with its significant coal base and good solar resource. It is therefore not surprising that Eskom issued a request for information (RFI) for solar boosting in October 2012 (Eskom, 2012b). The two main objectives of the RFI are to inform the Engineer Procure Construct (EPC) services of Eskom's intentions to roll out solar augmentation at Eskom sites, and to gather information on the capabilities of industry to achieve this.

The preheating of boiler feedwater with solar thermal energy is investigated in this work. Furthermore, SAPG is compared to stand-alone STPP. The 'tools' to undertake the investigation and comparison are developed in Section B.

Section B is sub-divided into two parts, namely a steady state thermal power plant model (Section 3) and a solar assisted power generation model (Section 4).

### 3. Steady State Thermal Power Plant Model

Most utility power plants utilize reheating and feedwater heaters, which employ regenerative measures. Typically, there are five to seven closed FWH's and one open FWH acting as the deaerator – three to four low pressure (LP) FWH's downstream and two to three high pressure (HP) FWH's upstream of the deaerator, as shown in Figure 6.

To investigate Regenerative Rankine cycles a simplified power plant was modelled. This was executed in MS Excel and limited to steady state.

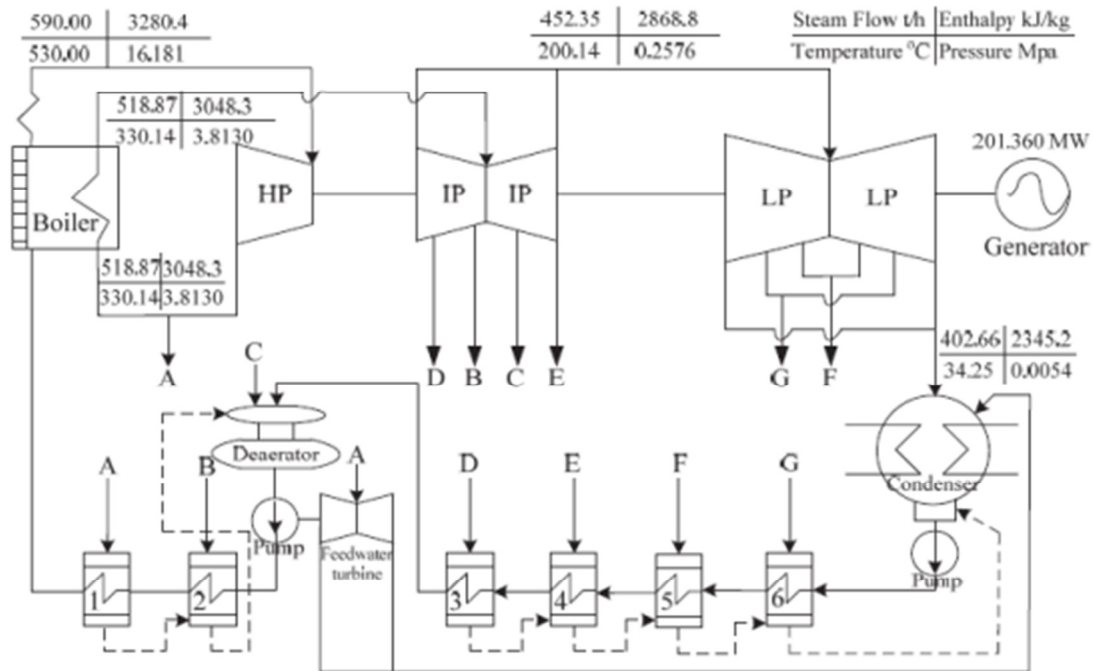


Figure 6: Schematic of a 200 MWel power plant (Yan *et al.*, 2010)

## 3.1 Modelling

### 3.1.1 Software tool

MS Excel was used to model steady state behaviour of a generic power plant. The freely available Excel add-in 'Water97\_V13' was used. This add-in allows the formulation of water and steam properties as authorised by the International Association for the Properties of Water and Steam (IAPWS). The forward equations are integrated into the Excel add-in. For example, the entropy and enthalpy are calculated by inputting temperature in Kelvin and pressure in bar absolute (bar). The backward equations are not incorporated; therefore, initially temperature could not be calculated from enthalpy or entropy with known pressure. The backward equations were programmed into the original add-in's Visual Basic source code – IAPWS documentation used for correlations (IAPWS, 2007). The program used to calculate water/steam properties was tested and verified with numerous test values provided.

### 3.1.2 Components

The following components which are standard to power plants with steam turbines were integrated into a whole-plant model:

- Boiler – with a furnace, waterwalls, drum(s), evaporative bank, superheater, reheater, economisers and air heaters
- Steam turbine – extraction condensing type with high pressure, intermediate and low pressure sections<sup>3</sup>
- Electrical generator – seen as a unit with a gearbox
- Condenser – heat exchanger between turbine exhaust steam and cooling water from cooling towers (either wet or dry)
- Feedwater system – feedwater pumps and heaters

A sequential approach is followed. The output of one component is taken as the input of the downstream component – no heat or pressure losses are taken for interconnecting piping. Heat and mass balances (HMB) are performed with efficiency analysis.

### 3.1.3 Description

The scenario selection inputs are given in Table 1, the state specifications in Table 2 and the component efficiencies in Table 3. In Table 1, the feedwater heating is set to 0 where no heating occurs and the boiler feedwater temperature equals the condenser outlet temperature plus the temperature rise over the pump and 1, the maximum value. For an infinite number of FWHs the optimal feedwater temperature is the saturated temperature of the boiler drum (Haywood, 1949). This is directly related to the pressure inside the drum, for instance at a 160 bar the saturation temperature is 347°C.

---

<sup>3</sup> Back pressure type steam turbines are typically used with cogeneration plants

**Table 1: Steady state thermal power plant model inputs – scenario selection**

Scenario inputs	options	value used (Section 3.1.3 example)
Reheating on/off	on or off	on
Feedwater heaters		
Number of FWH	1 - 7	2
Ratio of heating	0 - 1	0.3

**Table 2: Steady state thermal power plant model inputs - state specifications**

State inputs	value used
Boiler	
outlet steam temperature	550°C
outlet steam pressure	160 bar
reheat temperature	550°C
reheat pressure	40 bar
Condenser pressure	0.1 bar

**Table 3: Steady state thermal power plant model inputs - efficiencies**

Efficiency inputs	value used
Turbine isentropic	0.85
Pump isentropic	0.75
Heat exchanger (FWH)	0.95
Electrical generator (overall)	0.98



It should be noted that power plant efficiency mentioned thus far is thermal efficiency. For fuel to electric efficiency the boiler efficiency needs to be included. The boiler efficiency is inversely proportional to the outlet flue gas temperature (temperature at which flue gas (combustion gases) exits the boiler). A limitation to reducing this temperature to increase boiler efficiency is the dew point temperature. The dew point temperature is defined as the temperature at which the combustion gases are saturated with sulphuric acid (Singer, 1991). This establishes a corrosive environment and should be avoided. The dew point is proportional to the sulphuric acid content ( $\text{SO}_3/\text{H}_2\text{SO}_4$ ) which depends on the sulphur content of fuel.

The boiler feedwater is typically not heated to more than around  $250^\circ\text{C}$  (Singer, 1991, Kitto & Stulz, 1992) – although it can be raised higher for super and ultra-super-critical plants.  $250^\circ\text{C}$  was used as the limit to boiler feedwater temperature (bottom left quadrant in Figure 7 is valid in terms of boiler feedwater final temperature. For condenser pressure of 0.1 bar, the ratio of heating is graphically displayed in Figure 7. The ratio of heating is taken relative to the optimal feedwater temperature for an infinite number of FWHs, namely the saturated temperature of the boiler drum (in this case  $347^\circ\text{C}$ ). Note the ratio is calculated with enthalpy, hence not linear on temperature basis. In this case the ratio of heating is limited to 0.6 ( $250^\circ\text{C}$ ).

To describe the model, a basic reheat and regenerative Rankine cycle with two indirect feedwater heaters is used – refer to Figure 8. To display water/steam properties at various points in the power plant, the following information is provided: pressure in bar, temperature in  $^\circ\text{C}$ , enthalpy in  $\text{kJ/kg}$  and mass flow rate in  $\text{kg/s}$ . In Figure 9(a) – point t5 of Figure 8 is used. For steam extracted off the turbine, two additional properties are included, namely the saturation temperature and steam quality  $x$ , as shown in Figure 9 (b). The former is used for FWH calculations (described later in this section) and the latter needs to be monitored to ensure steam is of sufficient quality (not too ‘wet’) – typically above 0.9.

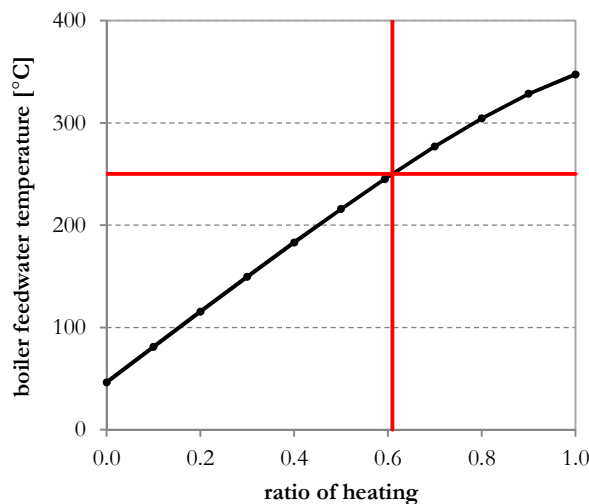


Figure 7: Graphical description of ratio of heating

The scenario inputs listed in Table 1 (right hand column) are used. To allow the mass flow rates to represent percentage values, the mass flow rate is taken as 100 kg/s. It should be noted that the model is linear and therefore efficiencies are not dependent on the power plant size.

*Boiler (b1 to t1)*

The output of boiler Superheater SH point t1 (top left of Figure 8) is taken as the starting point. The inlet temperature of the economiser is determined by the heating ratio, in this case 0.3 (boiler feedwater temperature of 150°C). The thermal input of the boiler, excluding the reheater, is calculated by simply taking the total enthalpy difference between the two stated points. For this model, part load behaviour of the boiler is not incorporated. The boiler (excluding reheater) heat input is calculated from:

$$q_{boiler,in} = (h_{t1} - h_{b1}) \tag{2}$$

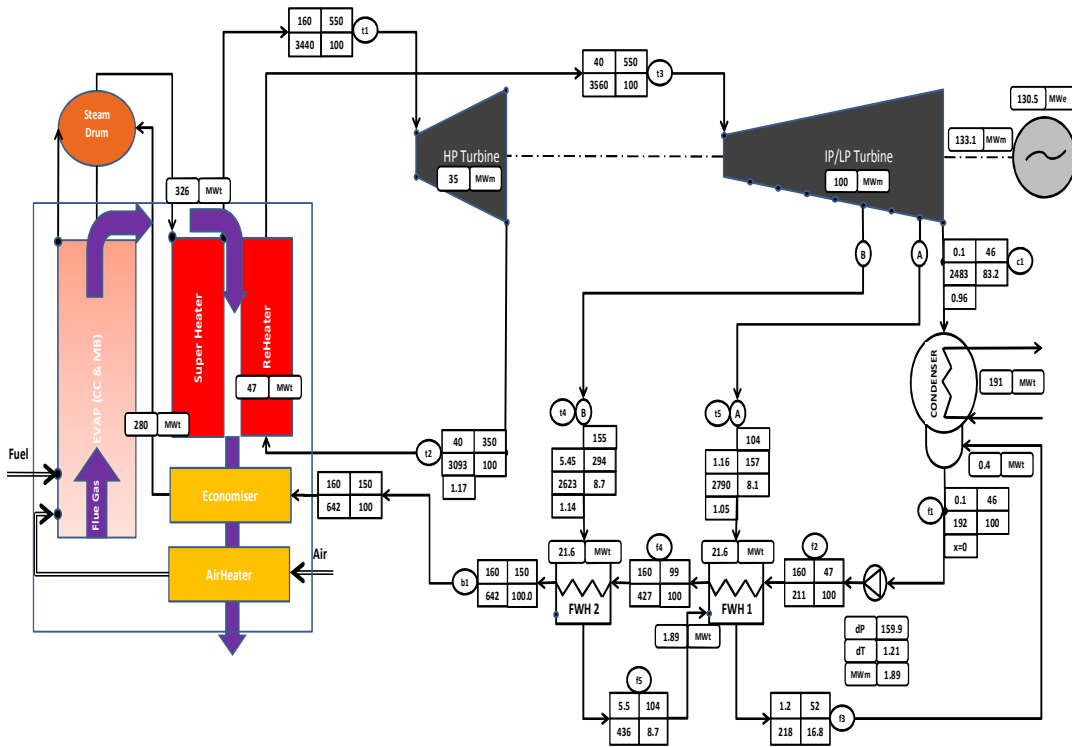


Figure 8: Schematic diagram of heat and mass balances of a generic power plant

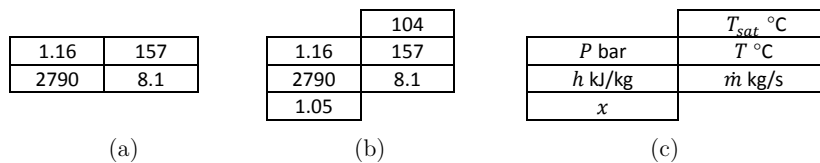


Figure 9: Water/steam property labels in (a) typical (b) extraction steam, and the units thereof (c)

*HP turbine (t1 to t2)*

To determine the isentropic efficiency  $\eta_{Turb}$  of the turbine, both high pressure (HP), intermediate (IP) and low pressure (LP) sections are taken as 0.85 (Table 3). It is acknowledged that the efficiencies typically increase with decreasing pressure sections – the LP section of turbine is more efficient than the HP section. For this investigation, a single/common isentropic efficiency is considered adequate for all stages. The turbine work output is determined by:

$$w_{TurbHP,out} = \eta_{TurbHP}(h_{t1} - h_{t2s}) \quad (3)$$

where  $h_{2s}$  is calculated with  $s_2 = s_1$  – refer to Figure 3

*Reheater (RH) (t2 to t3)*

RH pressure and temperature are taken as  $\frac{1}{4}$  of HP turbine inlet pressure (40 bar) and equal to the HP turbine inlet temperature (550°C) respectively. The reheater heat input is given as:

$$q_{RH.in} = (h_{t3} - h_{t2}) \quad (4)$$

*IP/LP turbine (t3 to t4, t5, c1)*

As mentioned, for optimal feedwater heating the enthalpy rise of each FWH is equal, therefore the outlet temperature of each FWH can be calculated. In this case, the inlet and required outlet temperature of the FWH system is respectively 47 and 150°C, therefore the intermediate temperature outlet for FWH1 is 99°C. The turbine work outputs are calculated in a similar manner to the HP section.

For extraction points t4 & t5 the pressures are determined by considering the required outlet temperature. To this outlet temperature, a temperature difference is added, in this case 5K. To this newly calculated temperature, the saturated temperature of extracted steam is related. For instance, with FWH1 the required outlet temperature is 99°C, therefore the extracted steam's saturated temperature needs to be 104°C (99 + 5). From this, the required extracted pressure is determined, namely 1.16 bar.

The mass flow rates of extracted steam are calculated – refer to *FWH system (f2 to b1)*. The remaining flow is condensed.

*Condenser (c1 to f1)*

The condenser pressure is taken as 0.1 bar. The outlet of turbine c1 is condensed to saturated liquid f1 ( $x = 0$ ). The FWH system is of the down cascading type (condensed extracted steam of FWH is feed to downstream FWH where sensible heat exchange occurs) with some of the condensed extracted steam being feed into the condenser. Therefore the condenser has to reject this sensible heat to the atmosphere – in this case 0.4 MW thermal. Condenser heat rejected is calculated as:

$$q_{cond.out} = (h_{c1} - h_{f1}) \quad (5)$$

with  $h_{f1}$  taken as saturated liquid enthalpy based on pressure (in this case 0.1 bar)

*FWH system (f2 to b1)*

Of specific interest in this section is the FWH heating system, namely two indirect feedwater heaters. The efficiency of the FWH is taken as 95%; therefore heat losses are accounted for. From the above information, the extracted steam mass flow rate can be determined. It should be noted that an iterative approach is required as the cascading effect needs to be incorporated. The outlet enthalpy of FWH1:

$$H_{f4} = H_{f2} + \eta_{FWH} \dot{m}_{t5} (h_{t5} - h_{f3}) + \eta_{FWH} \dot{m}_{f5} (h_{f5} - h_{f3}) \quad (6)$$

where  $h_{f3}$  is calculated by stipulating  $T_{f3} = T_{f2} + 5K$ . The calculations for FWH2 are similar but, in this case, no heating from the upstream cascade is included. The power plant thermal efficiency is calculated with:

$$\eta_{th} = \frac{w_{net}}{q_{in}} \quad (7)$$

with  $w_{net} = w_{turb.,out,total} - w_{pump,out,total}$  and  $q_{in} = q_{boiler,in} + q_{RH,in}$ . The former is simply the total turbine work minus the total pump work and the latter is the summation of heat inputs from the boiler (excluding reheater) and reheater.

### 3.2 Model validation

The model is a heat and mass balance exercise; therefore fundamental modelling is performed and should be inherently correct if the ‘accounting’ system is true. For realistic inputs and assumptions, the book ‘*Thermodynamics: An engineering approach*’, and specifically Chapter 9 (Cengel and Boles, 2002) was studied extensively. With reference to the literature and the author’s experience in HMB<sup>4</sup> a good comparison was found over a wide range of inputs, as shown in Figure 10 – where there is no reheating and the condenser pressure is taken as 29 mm Hg (0.04 bar). The data points (solid black markers) are referenced from a comprehensive eight volume series ‘*Modern Power Station Practice*’ (Sherry, 1971). Blue lines with hollow markers are model outputs.

---

<sup>4</sup> Direct comparison to commercial steam turbine suppliers’ HMB outputs were made

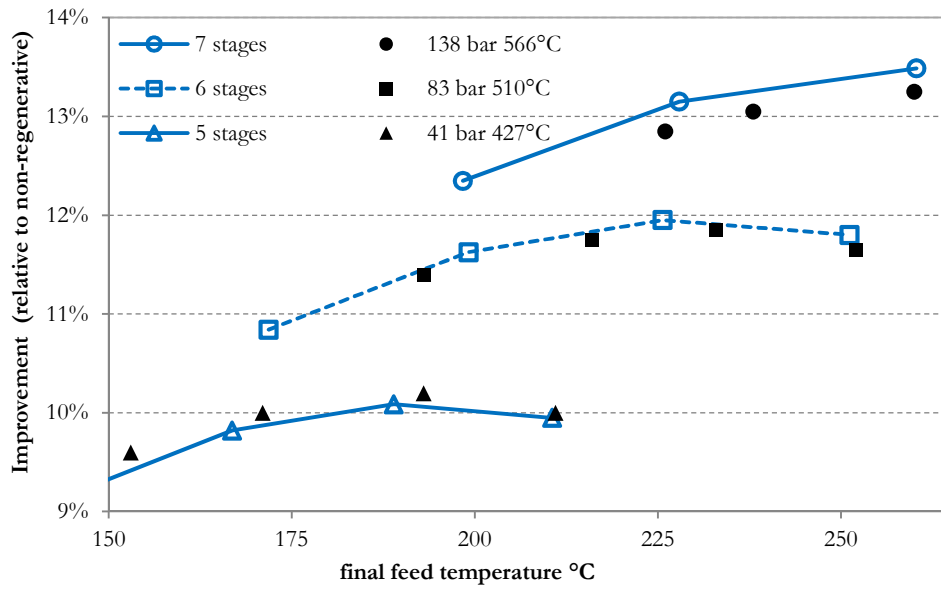


Figure 10: Improvement in thermal efficiency with feed water heating (no reheating (data points (blue markers) are referenced from Sherry, 1971))

The results of the steady state thermal power plant model are presented in Section 5.1.

## 4. Solar Assisted Power Generation (SAPG) Model

The previous model provided insight to the limitations of regenerative Rankine cycle and established a basis for solar assisted power plant modelling. The power plant model utilized in this section is based on a 600 MW electric subcritical fossil power plant – the specifications are presented in Figure 11. The Sealing Steam Recirculation (SSR) was considered negligible and neglected (less than 0.5% total steam mass rate) as well as the heating influence of the oil and hydrogen coolers, vent condenser, and air ejector/vacuum pump (less than 1°C heating).

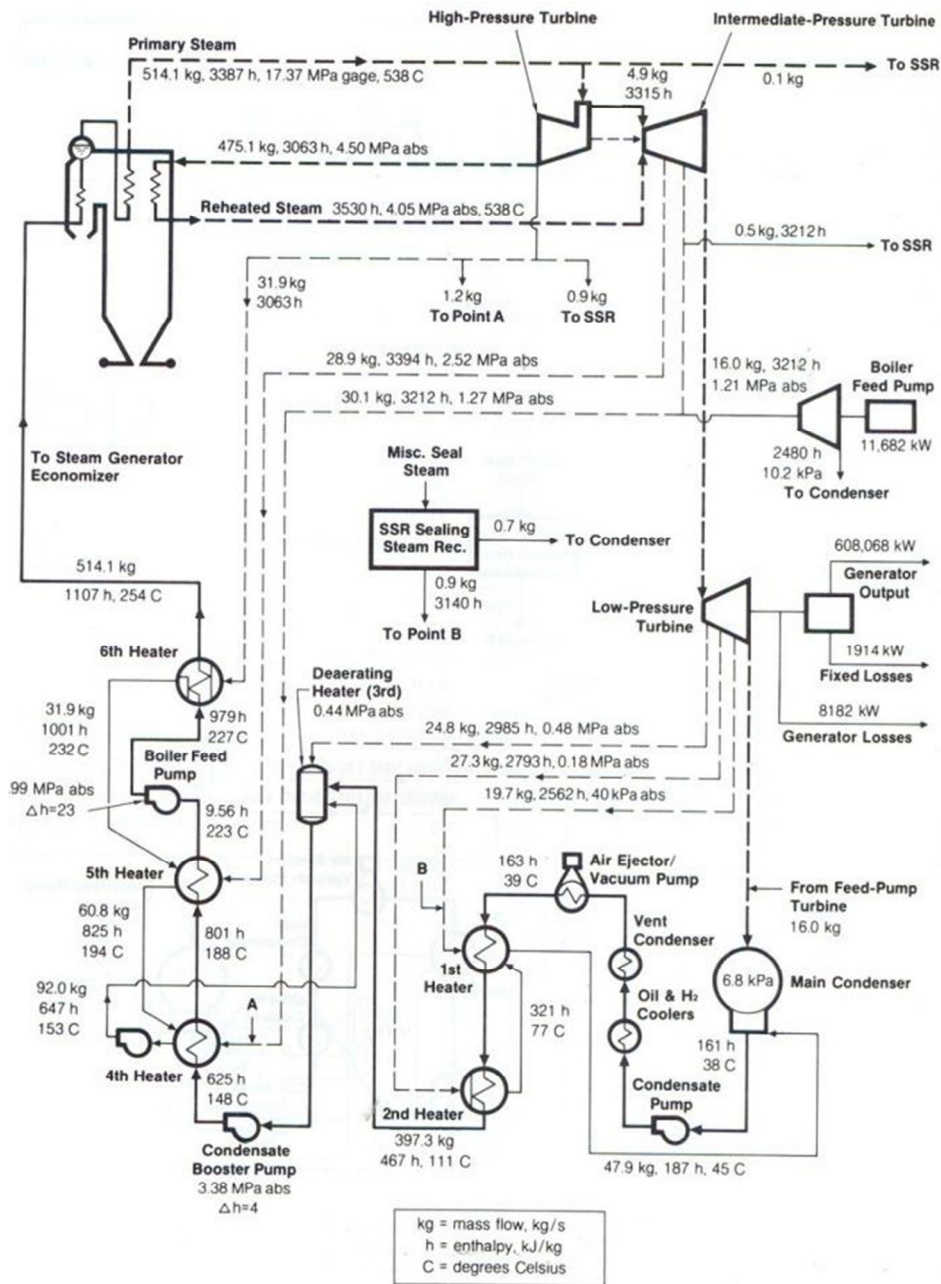


Figure 11: Reheat regenerative cycle, in a 600 MW subcritical fossil power plant (Singer, 1991)

## 4.1 Solar field

### 4.1.1 Software tool

With SAPG, solar fields generate process heat to replace bled-off steam in a conventional regenerative power cycle. The modelling of these solar fields was achieved with National Renewable Energy Laboratory's (NREL) System Advisor Model (SAM). SAM is a power plant modelling tool – an annual simulation consists of quasi-steady-state hourly calculations dependent on instantaneous weather conditions and the state of the plant from a previous time step. SAM was selected as it is a reputable tool and has capabilities to approximate transient behaviour of a solar field (due to intermittent solar resource). For a description of SAM models used, please refer to Wagner & Zhu, (2012) and SAM, (2009).

### 4.1.2 Solar field integration

There are two options for solar field integration into fossil fuel power plants, namely indirect and direct integration. Indirect integration requires an additional heat exchanger with a separate solar loop. With direct integration, the feedwater is heated directly in the solar field, as shown in Figure 12, System control is achieved with control valves CV1 and CV2. Additional pressure losses will occur over the solar field and a booster pump might be required. It is important that the solar field is integrated in parallel to the conventional feedwater heating system and therefore the dependency of the power plant operation on the solar field is reduced, with the solar field merely playing a complementary role. The direct arrangement is not seen to be problematic in terms of water treatment<sup>5</sup>. With modelling, the extracted steam mass flow rate is stipulated, however with solar augmentation any additional heating reduces the extracted steam required accordingly (constant heating over FWH).

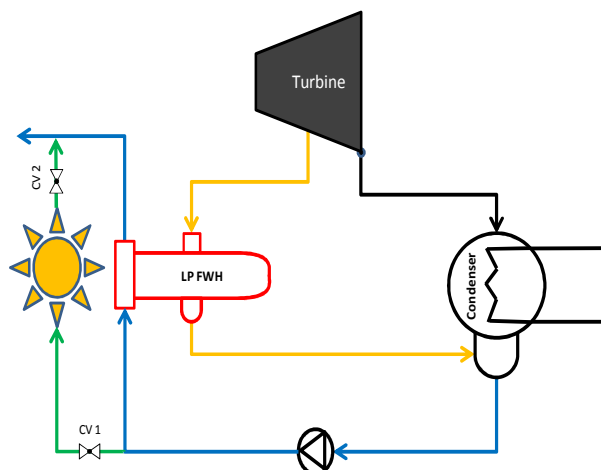


Figure 12: Direct integration of the solar field

<sup>5</sup> Personal communication with Denis Aspden, retired Eskom chemist, 22 October 2012

The deareator is an open FWH which performs oxygen removal. For this initial investigation, the extracted steam as an input to the deareator was not supplemented with solar heat. This FWH's operation was left as is. Further investigations to the possibilities of solar heating opportunities around the deareator are required (outside the scope of this study).

There are 6 FWHs. Since the deareator was not considered, 5 FWH stations are investigated, namely the 1<sup>st</sup>, 2<sup>nd</sup>, 4<sup>th</sup>, 5<sup>th</sup> and 6<sup>th</sup> stations shown in Figure 11 and Figure 13. The solar fields (SF) are named relevant to their associated FWH, for example SF1 supplements solar heat to FWH1 – refer to Figure 13.

#### 4.1.3 Solar collector technologies

The required temperatures of SFs are presented in Table 4. Four solar collectors are considered, namely flat plate (FP), evacuated tube (ET), Linear Fresnel (LF) and Parabolic Trough (PT)<sup>6</sup>. Collectors for the said temperature ranges are proposed.

**Table 4: Temperature ranges and investigated solar collectors**

solar field (SF)	approximate temperatures [°C]			proposed collectors			
	inlet	outlet	Average	FP	ET	LF	PT
1	40	70	55	X	X		
2	70	110	90	X	X		
4	145	185	165		X	X	X
5	185	220	205			X	X
6	225	250	240			X	X

<sup>6</sup> Compound Parabolic Collector (CPC) is not a commercial technology and hence omitted. The temperature ranges are easily obtainable with line focus solar collector technologies. For spatial and economic reasons, point focus technologies were not considered, hence Central Receiver (CR) was omitted



## 4.2 Modelling

### 4.2.1 Description

The same steady state thermal power plant model of energy efficiency section is utilized. The user inputs are similar, shown in Table 5 to Table 7; noteworthy changes are the condenser pressure is not taken as constant but related to atmospheric conditions ('dry' cooling)<sup>7</sup>, Eq 8, higher isentropic efficiency (0.88) for the LP turbine section than the HP/IP (0.85) and higher FWH heat exchanger efficiency of 0.99. For SAPG, the solar field model is described in the previous section. A graphical representation of the model is presented in Figure 13. The condenser pressure is calculated from:

$$P_{condenser} = P_{sat}(T_{db} + \Delta T) \quad (8)$$

where  $P_{sat}$  is the saturation pressure,  $T_{db}$  is the dry bulb temperature and  $\Delta T$  is taken as 15K. Ambient condition variation more closely resembles real conditions and has been shown to have substantial influence on power plant efficiency (Vosoogh & Hajidavalloo, 2010). Unless otherwise indicated weather conditions for Lephalale, Limpopo, South Africa (-23.68° (S), 27.75° (E))<sup>8</sup> are used as typical to the environment for utility power stations in South Africa. Weather files were generated with Meteororm (2010).

The plant was run in the solar booster mode. This has been shown to produce more rewarding results than in the fuel saving mode (Hu *et. al*, 2010) and assists Eskom's current generation expansion projects. This allows the boiler to run in a more stable mode and may provide assistance with accommodating peak electricity demand in the South African context, Figure 25. Solar assistance should not be problematic in terms of accommodating the additional mass flow through the turbine and efficiency variation occurs due to:

- Solar heating corresponds to periods of high solar radiation and thus, typically higher ambient temperatures which translates to higher condenser pressures (especially with dry cooling), hence higher turbine exhaust densities. Therefore, the volumetric flow rates are similar even though there is a higher mass flow rate with solar assistance. Furthermore, most modern power plants are capable of increased mass flow rates – around 10% above rated turbine output (Petrov *et al.*, 2012).
- The variation in turbine shaft output with solar assistance is limited – for all SFs on: less than 15 and 3% for respectively hourly peaking and annual total outputs. This effect on turbine efficiency is assumed to be insignificant and neglected.

---

<sup>7</sup> South Africa is a water scarce country and typically employs dry cooling (vs. wet) for utility power generation

<sup>8</sup> Lephalale is home to Matimba and Mudepi (currently being built) power stations

**Table 5: SAPG model inputs – scenario selection**

Scenario inputs	options
Reheating on/off	on
Number of FWH	6
Ratio of heating	0.6 ( $\approx 250$ °C)

**Table 6: SAPG model inputs - state specifications**

State inputs	value used
Boiler	
outlet steam temperature	538°C
outlet steam pressure	173.7 bar
reheat temperature	538°C
reheat pressure	45 bar
Condenser pressure	related to dry bulb temperature

**Table 7: SAPG model inputs - efficiencies**

Efficiency inputs	value used
Turbine isentropic	
HP/IP	0.85
LP	0.88
Pump isentropic	0.75
Heat exchanger (FWH)	0.99
Electrical generator (overall)	0.98

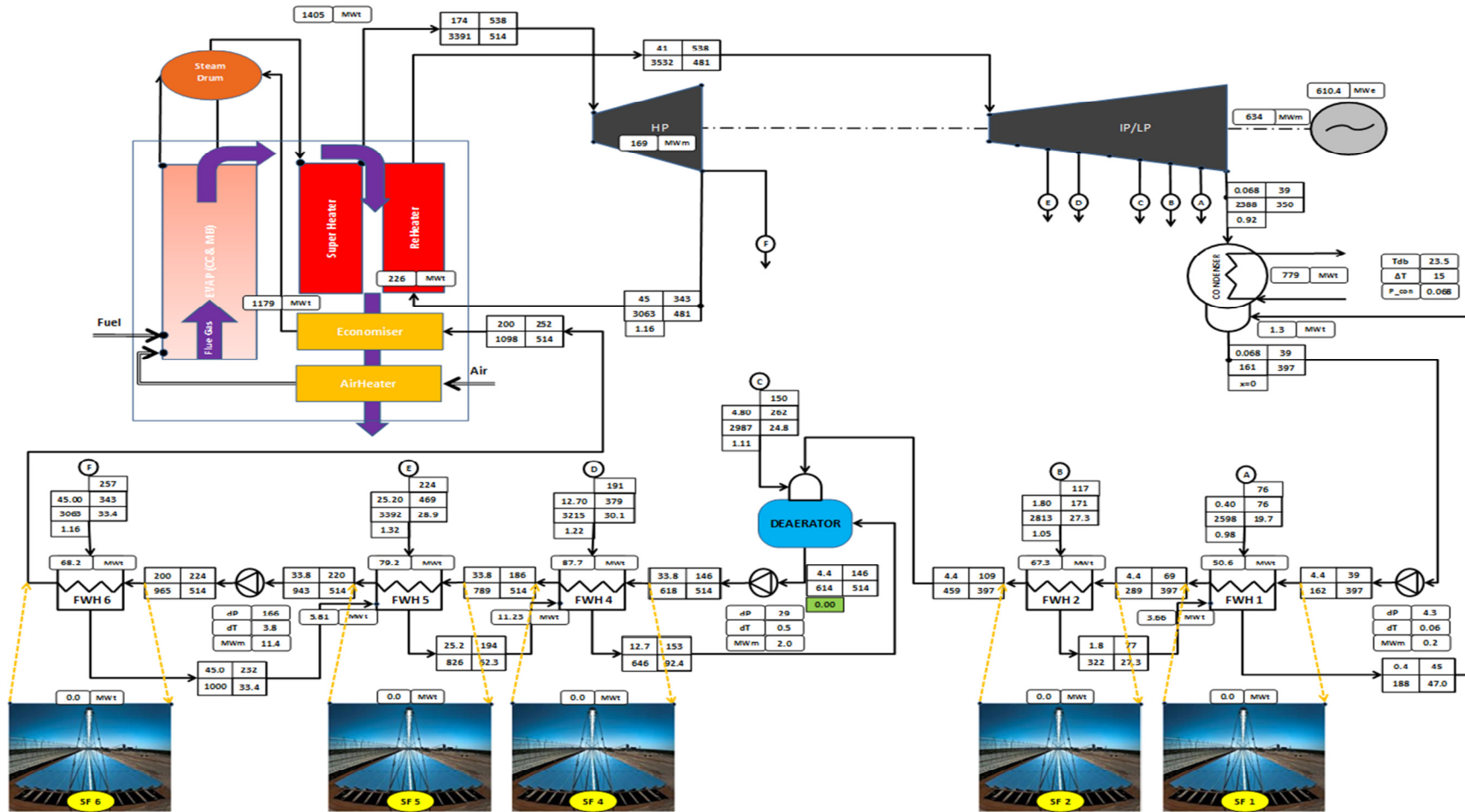


Figure 13: SAPG model representation (comparison to Figure 11 possible (solar off))

#### 4.2.2 Scenarios

Three scenarios are considered, namely:

- a) Various SFs
- b) Various solar collectors
- c) SAPG vs. stand-alone STPP

##### *Various SFs*

When considering the turbine extracted steam, for instance A to F in Figure 14, it is evident that two conflicting criteria are present. In terms of turbine setup it is more beneficial to supplement extracted steam at a higher stage or row. This, however, requires higher solar field outlet temperatures which typically translate to lower solar field efficiency and higher cost. It is worthwhile noting that supplementing extracted steam above reheat extraction point (HP exhaust) permits for secondary energy efficiency benefits in the form of greater reheating.

The individual solar fields were activated and corresponding solar boosting was recorded (one at a time). Solar boosting is considered as the additional electricity generated due to replacement of bled-off steam with solar process heat. To reduce computational time only one solar collector was used to compare various FWHs. The Linear Fresnel technology has been identified as a viable solution for solar process heat (IEA, 2005) and can operate at required temperate ranges. Additionally, the LF model in SAM allows for direct integration (DSG) as described in Section 4.1.2. A LF model with conventional N-S orientation was used as a base case.

The SF is sized at approximately 50 MW thermal. This was based on LF technology and equates to around 80 000 m<sup>2</sup> actual aperture area. SF heating is only activated if the solar field can provide more than 15% of heating capacity (7.5 MWh) over the hour considered.

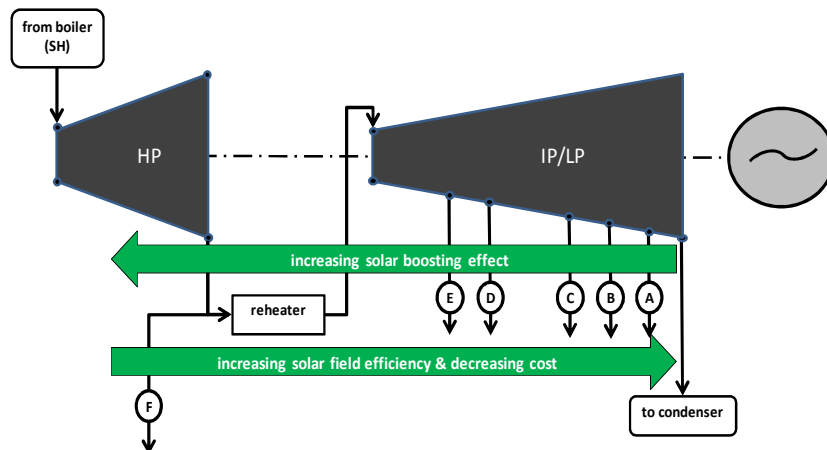


Figure 14: SAPG opposing 'forces'

### Various solar collectors

To allow comparison of other solar collectors, performance data was utilized, and is shown in Table 8. Efforts to source costs for collectors were problematic and were avoided. Only break even costs are provided.

The efficiency data presented in Table 8 is graphically shown in Figure 15 – the SFs are indicated with vertical lines. The efficiency  $\eta$  incorporates optical and thermal losses and is calculated with:

$$\eta = \eta_0 - a_1 \left( \frac{\Delta T}{G} \right) - a_2 \left( \frac{\Delta T^2}{G} \right) \quad (9)$$

with  $\Delta T = \frac{1}{2}(T_{SF,out} + T_{SF,in}) - T_{amb}$ ,  $G$  is the solar radiation [W/m<sup>2</sup>] and other constants are described in Table 8.  $T_{amb}$  and  $G$  were taken respectively as the average temperature during sunshine hours<sup>9</sup> (23°C) and average Direct Normal Irradiation (DNI)<sup>10</sup> (590 W/m<sup>2</sup>). For LF,  $\Delta T = (T_{absorber} - T_{amb})$  (Haberle *et al.*, 2002) with  $T_{absorber}$  assumed to be 50K above  $T_{SF,out}$  (outlet temperature of solar field).  $T_{SF,out}$  is used in the graph to indicate applicable solar collectors more clearly.

**Table 8: Summary of solar collector performance (Kalogirou, 2003)**

collector type	motion	concentration ratio	indicative temperature range [°C]	performance (efficiency) $\eta$		
				intercept efficiency $\eta_0$	1st order coefficient $a_1$ [W/m <sup>2</sup> K]	2nd order coefficient $a_2$ [W/m <sup>2</sup> K <sup>2</sup> ]
FP	stationary	1	30 - 80	0.8	4.78	--
ET	stationary	1	50 - 200	0.82	2.19	--
LF	1-axis tracking	10 - 40	60 - 400	0.61*	0*	0.00038*
PT	1-axis tracking	15 - 45	80 - 400	0.762	0.2125	0.001672

\*(Haberle, 2002)

<sup>9</sup> The average temperature and DNI for Lephalale are respectively 19°C and 260 W/m<sup>2</sup>. This would inaccurately represent the ambient conditions ‘experienced’ by solar field

<sup>10</sup> For stationary collectors the solar component Latitude Tilt Irradiation (LTI) or Global Horizontal Irradiation (GHI) should be used. It was assumed that DNI is representative and for simplicity, was used instead.

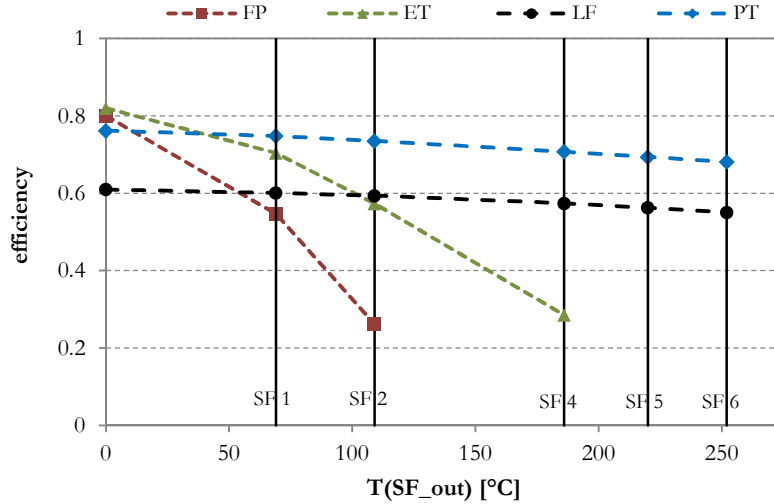


Figure 15: Solar thermal collector efficiency ( $G = 590 \text{ W/m}^2$ )

As expected the performance of non-concentrating collectors reduces considerably with increasing temperatures. PT is more efficient than LF over all temperatures considered – around 1.25 times. It should be noted that comparison was performed on aperture area and not land footprint. LF is more ‘compact’ than PT – about 20 to 30% lower due to denser mirror arrangement (Dersch *et al.*, 2009). If based on land footprint, PT’s lead over LF is reduced to around 1.2.

It should be noted that performance is given in terms of solar radiation normal to the collector. Non normal operation is quantified with Incidence Angle Modifiers (IAM) which are unique to each solar collector type. Therefore, the findings of this section are only indicative, for more comprehensive results refer to Section 5.

### ***SAPG vs. stand-alone STPP***

From findings of the previous two scenarios (results presented in Section 5.2.1 and 5.2.2), the most viable solutions are the concentrated solar technologies considered, namely PT and LF solar fields with N-S orientation providing process heat for FWH6 (final FWH). Recently with the Renewable Energy Independent Power Producers Programme (REIPPP) in South Africa, three CSP projects have been awarded – two Parabolic Trough plants and one Central Receiver plant. All three projects are located in the Northern Cape Province. As stated, Central Receiver technology was not considered for solar preheating applications due to economic and spatial constraints. Hence, the said SAPG at a power station, Figure 16, is compared to a stand-alone STPP plant in a good solar resource area, Figure 17. The SM for a stand-alone STPP plant was taken as 1 and the power block sized accordingly.

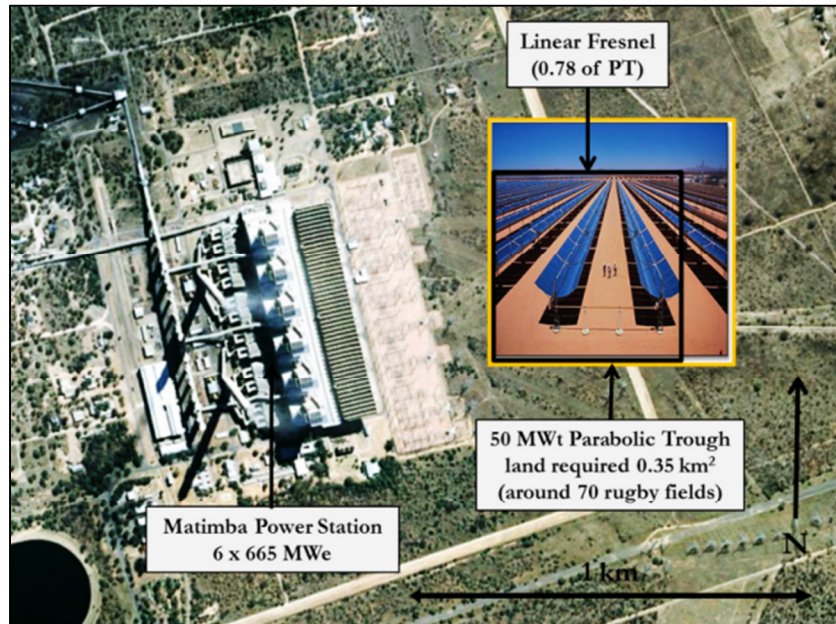


Figure 16: Relative size of the solar field to the Matimba power station

For a direct comparison the SF was taken ‘as is’. Furthermore, the same power plant specifications were used (thermal efficiency of 0.44 @  $P_{condenser} = 68$  kPa). It should be noted that this is a liberal estimate. The actual value is likely to be lower for stand-alone STPP due to, *inter alia*, unlike technologies (pulverised coal combustion vs. line focus solar collector) and different scales (utility (600 MWe) vs. industrial (25 MWe)). For instance, 0.44 thermal efficiency for a 25 MWe power block is optimistic. In short, from a SAPG perspective, the comparison is conservative.<sup>11</sup>

Upington, Northern Cape, South Africa (-28.42° (S), 21.26° (E)) is a well-known area for its good solar resource, specifically DNI for CSP – the proposed 5 GW solar park is intended to be located in the vicinity<sup>12</sup>. Weather files were generated with Meteonorm. The annual DNI for Upington is 20% greater than Lephale’s, the difference is less for GHI, Table 9. The average temperature is only considered for sunshine hours. Lower ambient temperatures are favourable for power generation efficiency.

Stand-alone STPP is a complete power plant – solar field, power block, balance of plant, etc. A SAPG plant is essentially a solar field integrated into a power plant. In terms of cost there are substantial benefits to SAPG. NREL developed a component-

<sup>11</sup> From calculations for stand-alone STPP with boiler outlet steam @ 400°C and 100 bar with reheater and 2 FWHs the thermal efficiency of power plant is approximately 0.37 @  $P_{condenser} = 68$  kPa. Therefore stand-alone STPP is around 15% less efficient (thermal to electric) than the utility power plant model used for SAPG. This is similar to data presented in Duffie & Beckman. (2006) for stand-alone STPP plant- efficiency of 0.376

<sup>12</sup> <http://www.energy.gov.za/SPark/default.html>

based cost model for parabolic trough solar power plants for use with SAM (NREL, 2010) – a cost assessment for a 103 MW Parabolic Trough with TES (dry cool option) is given in Table 10. For their assessment, a Solar Multiple (SM) of 2 was used. For the STPP stand-alone plant in Upington, no TES is assumed and hence the SM is reduced. With no TES, it is typical to have SM of slightly over 1, thus 1.1 is used. Values for SM = 1.1 are derived from SM = 2 costs and presented in the right column of the table. Breakdown of costs is portrayed in Figure 18. SAPG is 72% of the cost of a stand-alone STPP (PT) system (SM = 1.1 with no storage). This same ratio is assumed for LF.



Figure 17: Map of Southern Africa indicating the stand-alone STPP site (Upington) and the SAPG site (Lephalale) (Google Earth)

Table 9: Summary of weather conditions for investigated sites (Meteonorm, 2010)

location	DNI	GHI	Temperature
	annual total	annual total	average (sunshine hours)
	kWh/m <sup>2</sup>	kWh/m <sup>2</sup>	°C
Lephalale	2250	2100	22.8
Upington	2820	2280	25.4
difference	-20%	-8%	-2.6



**Table 10: Parabolic trough cost assessment (NREL, 2010), exchange rate used 1 USD = 9 ZAR (presented in thousands)**

Item	SM = 2			SM = 1.1 no storage	
	Material	labour	total		total
Site improvements	\$ 7 114	\$ 15 723	\$ 22 837	R 205 533	R 205 533
Solar field	\$ 212 135	\$ 284 253	\$ 496 388	R 4 467 492	R 2 457 120
HTF system	\$ 53 280	\$ 56 749	\$ 110 029	R 990 261	R 544 643
TES	\$ 202 638	\$ 5 438	\$ 208 076	R 1 872 684	--
Power block	\$ 112 136	\$ 39 057	\$ 151 193	R 1 360 737	R 1 360 737
EPCM costs			\$ 29 001	R 261 009	R 261 009
Project, land, misc			excluded	excluded	excluded
<b>Total</b>	<b>\$ 587 303</b>	<b>\$ 401 220</b>	<b>\$ 1 017 524</b>	<b>R 9 157 716</b>	<b>R 4 829 043</b>

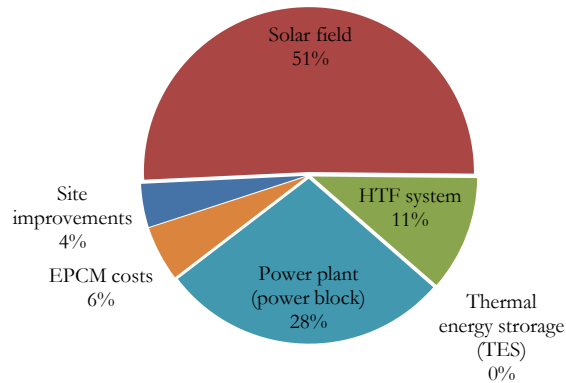


**Figure 18: Cost breakdown of a Parabolic Trough power plant**

### 4.3 Model validation

The outputs of the power plant model compares favourably to results found in literature – refer to Section 3.2 and Table 11. Efforts to accurately represent the behaviour of an actual power plant were attempted. For simulations performed this was adequately achieved in steady state conditions. Transient effects are outside the scope of this work.

The SF's were simulated in SAM, namely the Linear Fresnel and Parabolic Trough (empirical model). For validation of these models please refer to work by Wagner (2012) and Price (2003), respectively.

**Table 11: Comparison of outputs from literature and developed model**

	Feed water temperature [°C]			Net electricity generated [MWel]
	Outlet FWH2	Inlet FWH 4	Inlet boiler	
Figure 11 (Singer, 1991)	111	148	254	608
Model used	109	146	252	610
difference				<b>0.33%</b>

## 5. Results

An investigation of SAPG was performed, specifically when applied to the preheating of boiler feedwater. This section presents the results of simulations as described in Section B pertaining to SAPG explicitly. A similar format as Section B is followed, namely:

- Steady state thermal power model plant (regenerative measures)
- SAPG
  - Various SFs
  - Various solar collectors
  - SAPG vs. stand-alone STPP

### 5.1 Steady state thermal power plant model (regenerative measures)

The thermal efficiency of a 600 MW electric subcritical (160 bar superheated steam at 550°C) fossil powered power plant with a single reheater and without regenerative heating was calculated as 0.38 @  $P_{condenser} = 100$  kPa. Preheating of boiler feedwater with extracted steam from the turbine shows significant improvements with diminishing returns with additional number of FWHs, Figure 19. For a 7 stage FWH system raising the final feed temperature to 245°C, an improvement of around 11% is achieved with 30% of turbine inlet steam being extracted. The effects of boiler feedwater preheating is shown in Figure 20 (non-regenerative vs. regenerative). The values are relative to the respective heat source totals, for instance if 100 units of heating (heat source – total) are provided with non-regenerative cycle then 38 units of total turbine shaft output (turbine – total) are generated, hence 38% efficiency.

With regeneration, steam is extracted off the turbine to preheat boiler feedwater. Essentially, heat which was to be rejected to the atmosphere is now used for heating and thus waste is reduced. This is a more efficient use of energy. A further degree of this energy efficiency measure is cogeneration.

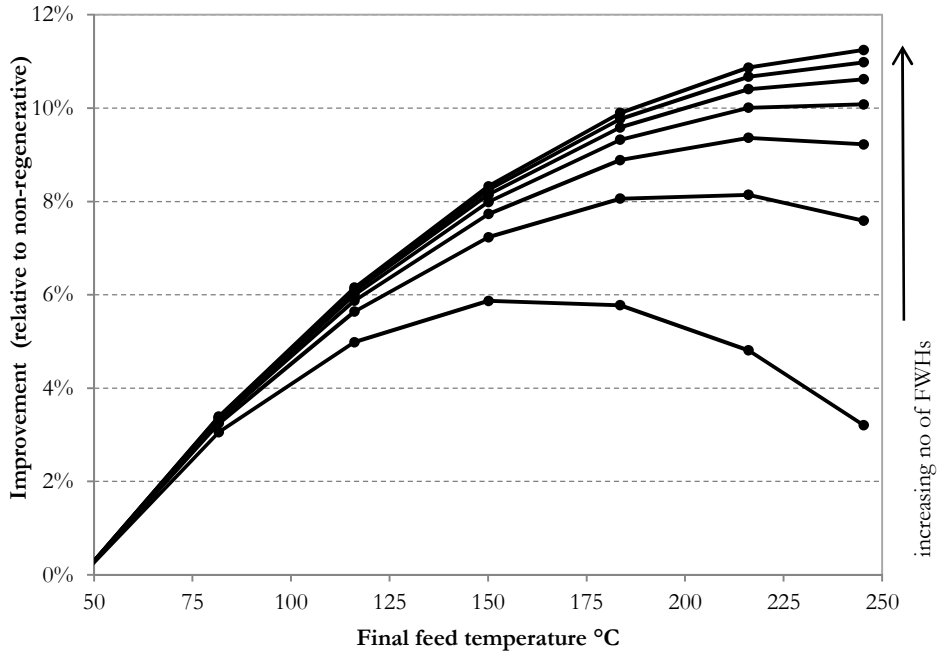


Figure 19: Efficiency improvements with preheating of boiler feedwater

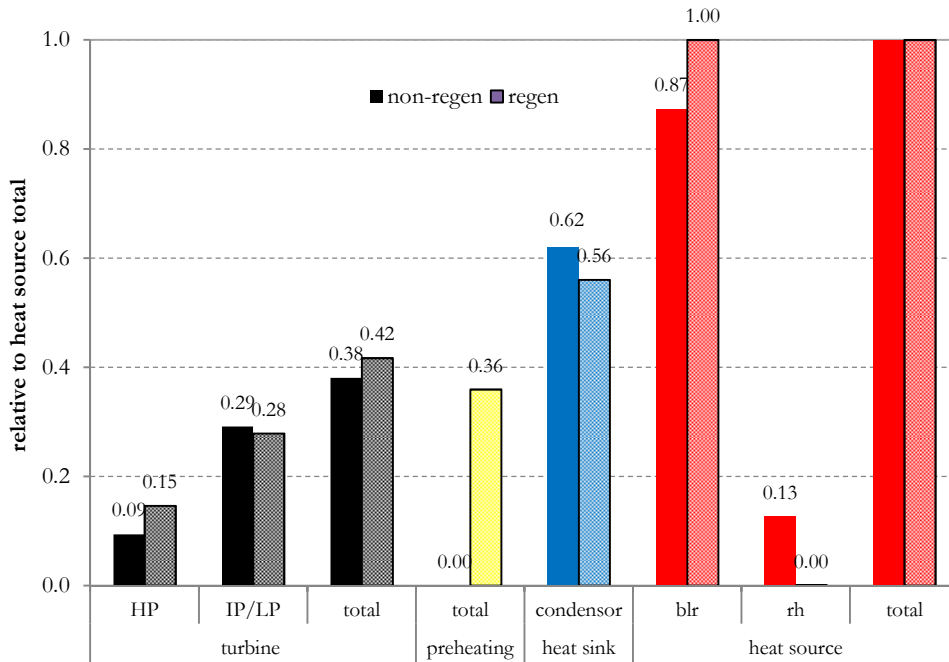


Figure 20: Effect of regenerative heating

## 5.2 SAPG

### 5.2.1 Various SF

A 50 MW thermal LF SF (approximately 80 000 m<sup>2</sup> aperture area) with conventional N-S orientation was used as a base case to investigate various feed-in points, namely different FWHs – refer to Figure 13. Annual simulations with hourly weather data were executed. The efficiencies are shown in Figure 21, giving the annual totals. As expected there is a reduction in solar field efficiency with increasing average temperature of solar field  $T_{SF,avg}$ . The thermal to electric efficiency increases significantly with increasing average temperature of the solar field  $T_{SF,avg}$  and resulting overall solar to electric efficiency increases. This trend was also found by Siros *et al.* (2012). For SF6 the supplemented extraction steam allows additional reheating. This further benefit is seen between SF5 and SF6. The solar to electric efficiency for all SFs are superior to stand-alone STPP at similar temperatures. SF6 at slightly over 20% annual solar to electric efficiency is superior to a typical stand-alone line focus STPP (for instance SEGS VIII solar to electric efficiency of 14% (NREL, 2008)).

### 5.2.2 Various solar collectors

It is evident that SF6 is superior to other solar assistance integration points when considering LF technology. To investigate further solar collectors the results of the previous section are incorporated with findings of Section 4.2.2 (Figure 15). Initially, the comparison is limited to normal incidence of irradiation (the sun in an optimal position, such as directly above the horizontal collectors). The influence of non-normal incidence is presented subsequently.

The relative performance (solar boost) for flat plate (FP), evacuated tube (ET) and Parabolic Trough (PT) are compared to Linear Fresnel (LF) at SF6, and shown in Figure 22. Non-concentrating technologies are not competitive. This is evident as thus far only concentrating technologies have been employed for feedwater heating. An example is the currently constructed LF solar booster for the supercritical Kogan Creek power plant discussed in Section 2.2. From these findings, in terms of feedwater heating, LF needs to be around 75% of the installation cost of PT to be cost effective.

For non-normal incidence angles, annual simulations were limited to PT and LF at SF6. The actual aperture area of around 80 000 m<sup>2</sup> was used. The monthly additional electric output (solar boost) is presented in Figure 23. A comparison of North-South (N-S) and East-West (E-W) orientation of the solar field is also included. The representative annual totals are shown on the right. On equal aperture area basis, PT outperforms LF significantly. On annual total basis PT is more than 30% and almost 50% greater than LF for respectively N-S and E-W orientation. For conventional N-S arrangement LF needs to be around 53% of the specific installation costs (in \$/m<sup>2</sup> aperture area) of PT in order to be cost competitive. This is similar to findings by Morin *et al.* (2012), Giostri *et al.* (2011) and Dersch *et al.* (2009).

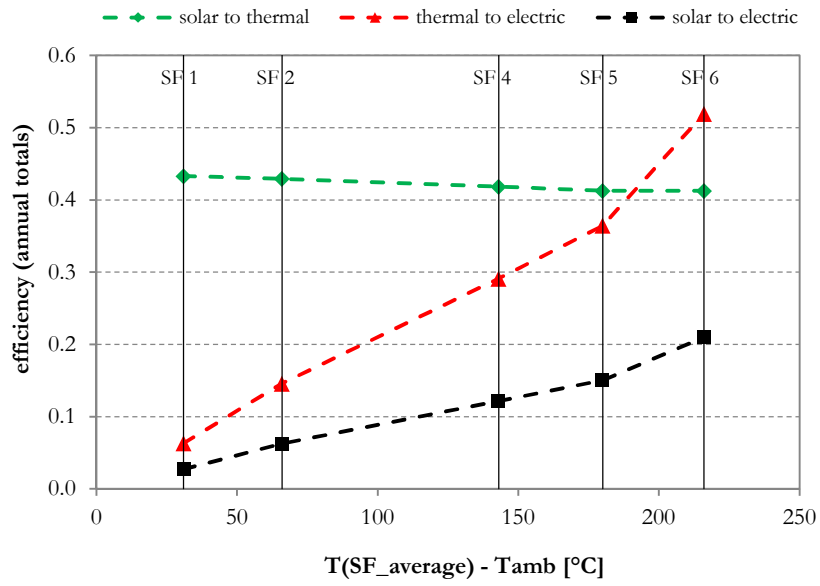


Figure 21: Annual total efficiencies for various solar field integrations

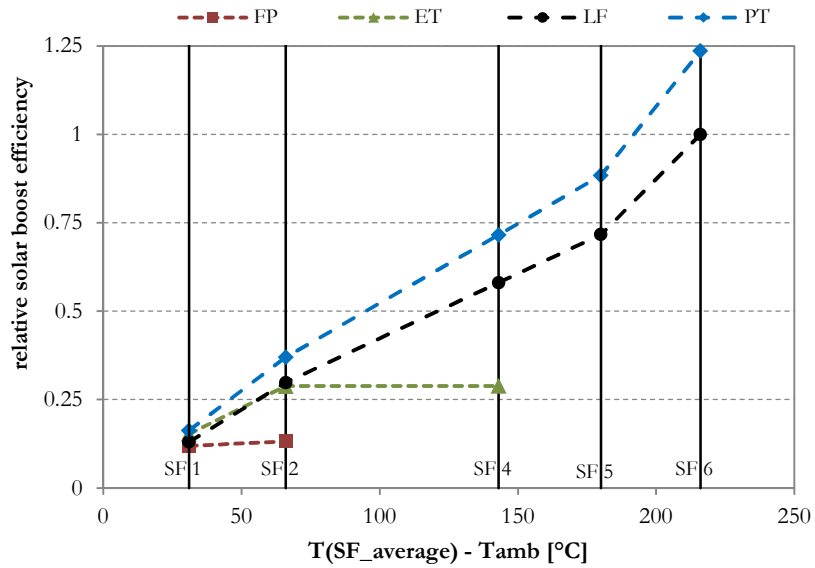


Figure 22: Performance per cost comparison for various solar collectors (relative to LF at SF6)

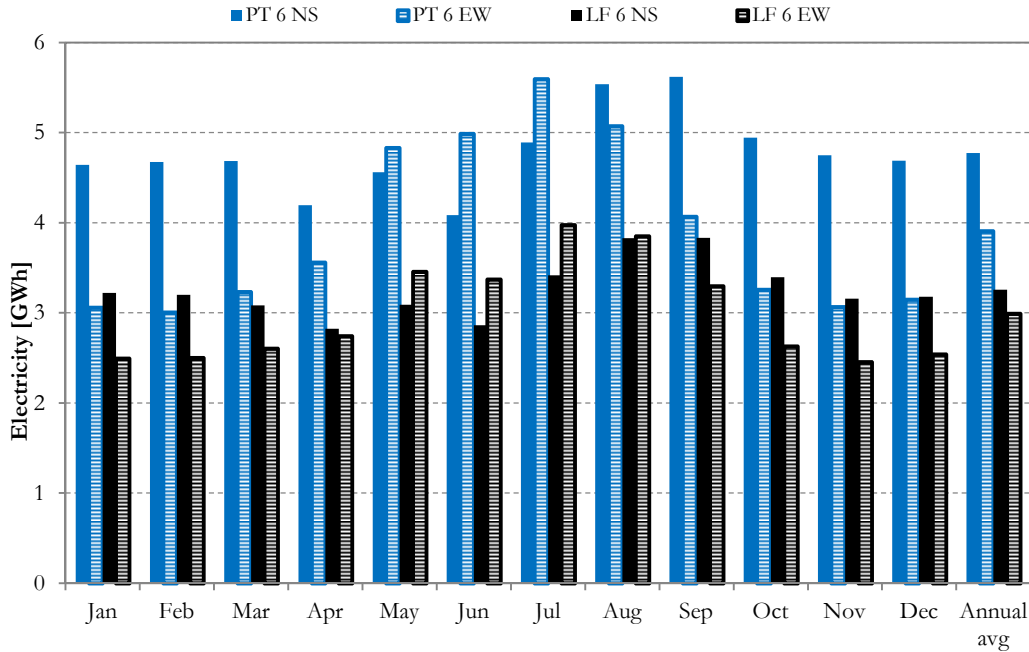


Figure 23: Performance comparison of parabolic trough and linear Fresnel (SF 6)

The reasons for the vast difference is, *inter alia*, higher optical efficiency used (PT = 0.75 to LF = 0.64)<sup>13</sup> and better inherent ‘optical tracking’ capabilities of PT. The latter is best displayed with Incidence Angle Modifiers (IAM); IAM provide the ratio of transmittance-absorptance product at some angle relative to transmittance-absorptance product at normal irradiance. See the simulated results from Morin *et al.* (2011) in Figure 24. With PT, the reflectors (trough) are normal to the sun in terms of the transversal plane, therefore transversal IAM  $\theta_t$  is 1 (unity) except for large incidence angles due to shading of rows (in this case above 70°). For longitudinal IAM  $\theta_i$ , PT and LF are similar. The tracking capabilities in the transversal plane for PT are superior to LF. This is shown with annual average differences in Figure 23 (right).

The influence of IAM is depicted by considering a clear summer day, Figure 26, and a clear winter day, Figure 27. An N-S arrangement is used, therefore for E-W arrangement  $\theta_t$  becomes  $\theta_i$  and *vice versa*. For winter day the dip in SF output for PT N-S coincides with high  $\theta_i$ .

SAPG might be appropriate for ‘peaking’ electricity generation. For this to be realized the output of solar boosting needs to coincide with electricity demand, as shown in Figure 25. This could be achieved with SF in terms of collector technology, field orientation and/or Thermal Energy Storage (TES). An example of such a consideration is favouring E-W orientation of SF rather than conventional N-S at the expense of less total annual solar boosting but greater output in winter months, depicted in Figure 23.

<sup>13</sup> Default values in SAM used

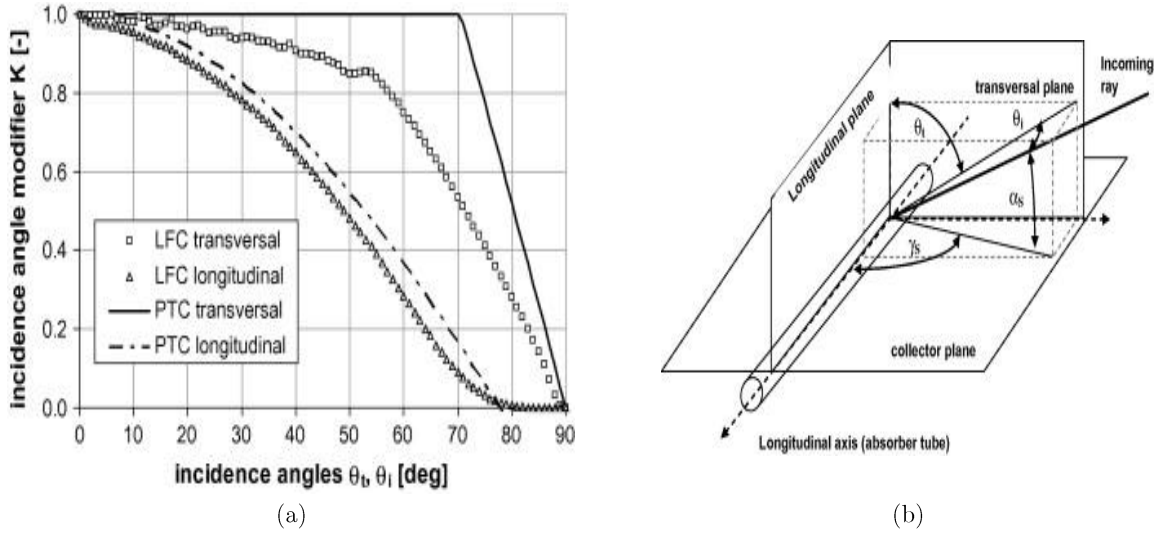


Figure 1: (a) Simulated incidence angle modifiers for Parabolic Trough and Linear Fresnel (b) definitions used:  $\theta_t$  is transversal IAM and  $\theta_i$  is longitudinal IAM (Morin *et al.*, 2011)

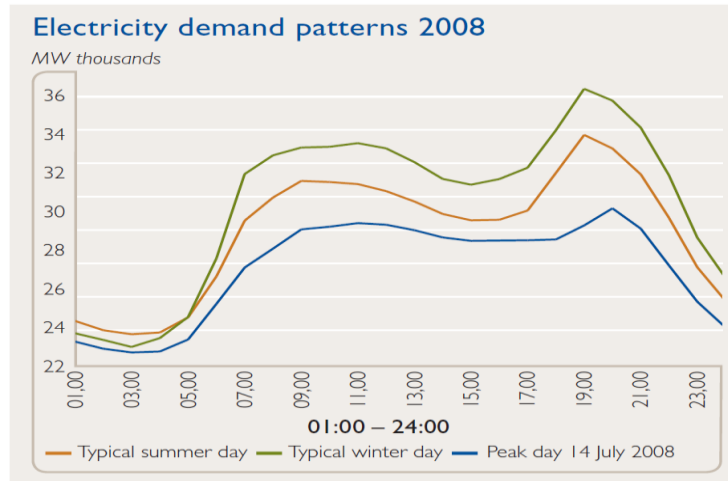


Figure 2: Average national electricity demand for South Africa (Eskom, 2009)



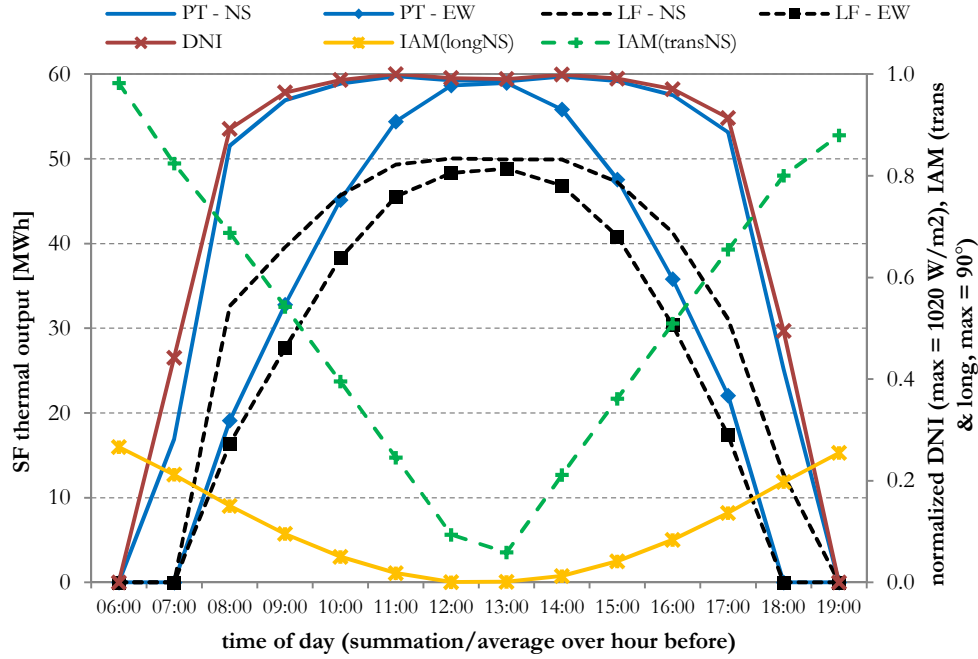


Figure 26: Solar thermal output from SF - clear summer day (20 December)

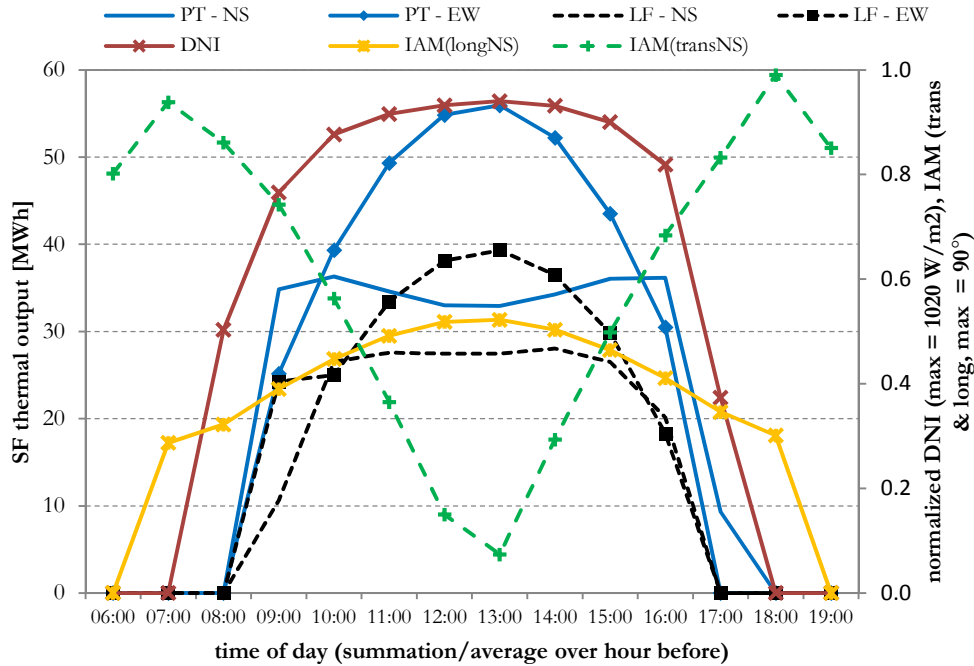


Figure 27: Solar thermal output from SF - clear winter day (19 June)

### 5.2.3 SAPG vs. stand-alone STPP

From findings of the previous two scenarios, the most viable solutions are the concentrating solar technologies considered, namely PT and LF solar fields with N-S orientation providing supplementing heating to FWH6 (final FWH). SAPG at a power station in Lephalale is compared to a stand-alone STPP plant in a good solar resource area, namely Upington. Two PT STPP plants in the Northern Cape were recently awarded with REIPP. Thus the solar collector technology considered is PT. For details refer to Section 4.2.2.

The flow of energy, namely solar radiation on the solar field (solar field inlet), the solar field thermal output (solar field outlet) and the electricity generated for stand-alone STPP and SAPG are compared in Figure 28 and annual totals are given. Due to a higher DNI annual total of the good solar resource area, the solar field inlet for SAPG is 0.8 of STPP. Due to higher thermal losses with STPP solar field's elevated temperatures, the solar field outlet difference is reduced (solar field efficiencies (annual) of 50 and 58% respectively for STPP and SAPG). Ultimately, the annual electricity generated with SAPG out performs stand-alone STPP by more than 25%. Gupta & Kaushik (2009) found SAPG (preheating of feedwater) to be around a 1.5 times more efficient use of solar thermal energy than stand-alone STPP. These findings are for the same site and therefore equal solar resource. If 20% more annual DNI total at stand-alone STPP site is factored in, then the findings are similar.

In Section 4.2.2, it was found that SAPG is 72% of the cost of a stand-alone STPP (PT) system ( $SM = 1.1$  and no storage). Therefore, a solar assisted HP feedwater heater system (SAPG) at an existing power plant is 1.8 times more cost effective than a stand-alone STPP (PT) in a good solar resource area. This is in line with expectations from an expert in the field of solar energy (Philibert, 2012)<sup>14</sup>. Furthermore, SAPG better performs in high electricity demand months (South African winter – May to August), shown in Figure 29.

---

<sup>14</sup> Author of 2010 IEA – CSP Roadmap, currently with ADEME, France

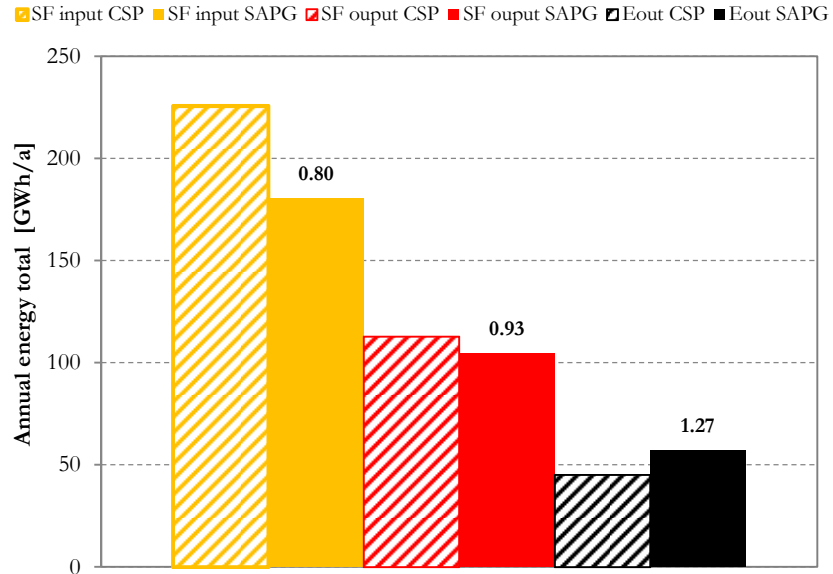


Figure 28: Energy breakdown of annual totals for stand-alone STPP and SAPG

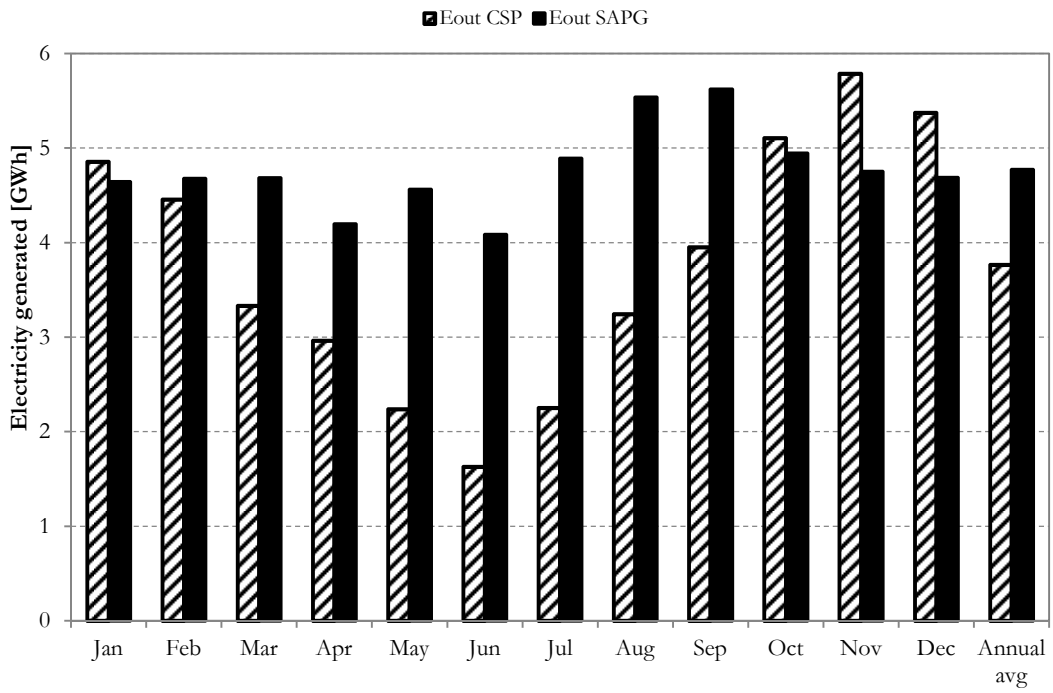


Figure 29: Comparison of electricity generated for stand-alone STPP and SAPG

## 6. Conclusions

An investigation of SAPG was performed; specifically solar preheating of feedwater. Feedwater heating provides significant improvements with diminishing returns with additional number of feedwater heaters (FWHs). For a 7 stage FWH system raising the final feed temperature to 245°C an improvement of around 11% is achieved with 30% of turbine inlet steam being extracted.

Power plant simulations were performed incorporating weather data for Lephalale, South Africa (Matimba power station). With an increase in solar augmentation (supplement extracted steam with solar heat), of the field's temperature, an increase in overall solar to electric efficiency was observed. The solar to electric efficiency for all SFs is superior to stand-alone STPP at similar temperatures. SF6 (final FWH) at slightly over 20% annual solar to electric efficiency is achieved at a solar field outlet temperature of around 250°C.

The performance of flat plate (FP), evacuated tube (ET), Linear Fresnel (LF) and Parabolic Trough (PT) solar collector technologies were compared. This comparison was limited to normal incidence of irradiation. For this application, non-concentrating technologies are not competitive.

For non-normal incidence angles, annual simulations were limited to PT and LF at SF6. The actual aperture area of around 80 000 m<sup>2</sup> was used (50 MW thermal based on LF). On equal aperture area basis, PT outperforms LF significantly. For a conventional N-S arrangement, LF needs to be around 53% of the specific installation cost (in \$/m<sup>2</sup> aperture area) of PT to be cost competitive

The suitability of SAPG for 'peaking' electricity generation was discussed. With deliberation of SF in terms of collector technology, field orientation and/or Thermal Energy Storage (TES) peaking capabilities could be achieved. An example of such a consideration is favouring E-W orientation of SF rather than conventional N-S at the expense of less total annual solar boosting but greater output in winter months.

SAPG at Lephalale was compared to a stand-alone STPP in a good solar resource area, namely Upington, South Africa - PT solar collectors were utilized for both sites. Ultimately, the annual electricity generated with SAPG is more than 25% greater than stand-alone STPP. If SAPG is taken as 72% of the cost of stand-alone STPP, this translates to SAPG being 1.8 times more cost effective than stand-alone STPP. Furthermore, SAPG better performs in high electricity demand months (winter months in South African context).

Stand-alone STPP have been adopted in South Africa and are currently being built. This was achieved by government creating an attractive environment for Independent Power Producers (IPPs). On a national/Eskom level, SAPG, specifically solar preheating of feedwater, is a more viable solution for South Africa with its significant coal base and good solar resource.

## 7. Recommendations

It is recommended that work on part load behaviour prediction of power plants by Mavromatis & Kokossis (1998) be incorporated to more accurately model power plant performance. Ultimately, to investigate the actual behaviour of a power plant, and specifically the response to variations, a transient model is required. This was beyond the scope of this work. A simulation tool such as Flownex has been utilized for such purposes in other research work.

Further investigations into the effect of temperature levels and site location on solar field performance are recommended. These factors need to be isolated for a better understanding of solar field performance prediction. Furthermore, the trade-off between more advanced absorbers and the associated increased costs thereof could provide insight into lower cost solar collector technologies options, specifically for solar process heat.

Thermal Energy Storage (TES) for the stand-alone STPP was not considered. Storage allows for better utilization of the power block and typically reduces the Levelized Cost of Electricity (LCOE). TES for stand-alone STPP should be included in further research. If storage is not prescribed then stand-alone Photovoltaic plants should also be considered.

As CSP is still in early state of commercialization, especially Linear Fresnel (Richter, 2012) cost estimations of solar collector technologies were problematic to obtain. However, cost is the driving factor and further efforts should be applied here. Collaboration with industry is a viable means to further this research.

## List of References

- Cengel, Y.A. & Boles, M.A. 2002, *Thermodynamics: An engineering approach* 4<sup>th</sup> edition, McGraw Hill Publishers
- Dersch, J., Morin, G., Eck, M. & Haberle, A. 2009, Comparison of Linear Fresnel and Parabolic Trough collector systems – systems analysis to determine break even costs of Linear Fresnel, *Proceedings of SolarPACES 2009, 15 – 18 September 2009, Berlin, Germany*
- Duffie J.A. & Beckman, W.A. 2006, Solar engineering of thermal processes 3<sup>rd</sup> edition, John Wiley and Sons, Inc. Publishers
- Eskom, 2009, *Annual Report 2009*
- Eskom, 2012a, *Integrated Report 2012*
- Eskom, 2012b, *Request for information for Solar Boost*, RFI reference number: CORP 2371
- Giostrì, A., Binotti, M., Silva, P., Macchi, E. & Manzolini, G. 2011, Comparison of two linear collectors in solar thermal plants: Parabolic Trough vs. Fresnel, *Proceedings of the ASME 2011 5<sup>th</sup> International Conference on Energy Sustainability, 7 – 10 August 2011, Washington, USA*
- Gupta, M.K. & Kaushik. S.C. 2010, Exergy analysis and investigation of various feed water heater of direct steam generation solar-thermal power plant, *Renewable Energy* 35 (2010) 1228 – 1235
- Haberle, A., Zahler, C., Lerchenmuller, H., Mertins, M., Wittwer, C., Trieb, F. & Dersch, J. 2002, *Proceedings of SolarPACES 2002, 4 – 6 September 2002, Zurich, Switzerland*
- Habib, M.A., Said, S.A.M. & Al-Zaharna, 1999, Thermodynamic optimization of reheat regenerative thermal-power plants, *Applied Energy* 63 (1999) 17 – 34
- Haywood, R.W. 1949, Generalized analysis of the regenerative cycle, *Proc. I. Mech. E.*, vol. 161, p. 157
- Hu, E., Yang, Y., Nishimura, A., Yilmaz, F. & Kouzani, A. 2010, Solar thermal aided power generation, *Applied Energy* 87 (2010) 2881 – 2885
- IAPWS, 2007, *Revised release on the IAPWS industrial formulation 1997 for the thermodynamic properties of water and steam*
- IEA, 2005, *Medium Temperature Collectors*, IEA SHC – Task 33
- IEA, 2012, *Key World Energy Statistics 2012*

- Kalogirou, S. 2003, The potential of solar industrial process heat applications, *Applied Energy* 76 (2003) 337 - 361
- Kitto, J.B. & Stultz, S.C. 1992, *Steam: its generation and use*, 41<sup>st</sup> edition, The Babcock and Wilcox Company
- Kogan Creek Solar Boost Project, 2012, Available from <http://kogansolarboost.com.au> [September 2012]
- Mavromatis, S.P. & Kokossis, A.C. 1998, Conceptual optimisation of utility networks for operational variations – I. Targets and level optimisation, *Chemical Engineering Science* Vol. 53, Issue 8, 1585 - 1608
- Morin, G., Dersch, J., Platzer, W., Eck, M. & Haberle, A. 2012, Comparison of Linear Fresnel and Parabolic Trough collector power plants, *Solar Energy* 86 (2012) 1 - 12
- Meteonorm, 2010, *Meteonorm Version 6.0 Handbook part II: Theory*
- Novatec Solar, 2012, Available from <http://www.novatecsolar.com/8-1-Projects.html> [September 2012]
- NREL, 2008, *TroughNet: Solar parabolic power network*
- NREL, 2010, Parabolic Trough reference plant for cost modelling with the Solar Advisor Model (SAM), *Technical Report NREL/TP-5550-47605 July 2010*
- Paul, C., Teichrew, O., Ternerde, A. & Mills, J. 2012, Operational experience of the integration of a solar boiler based on Fresnel collector technology into a coal-fired power station, *Proceedings of SolarPACES 2012, 11 - 14 September 2012, Marrakech, Morocco*
- Petrov, M.P., Popa, M.S. & Fransson, T.H. 2012, Solar Augmentation of conventional steam plants: From system studies to reality, *Proceedings of WREF 2012, 13 - 17 May 2012, Denver, USA*
- Philibert, C. 2012, Personal communication 29 November 2012
- Price, H. 2003, A Parabolic Trough solar plant simulation tool, *Proceedings of ISES 2003, 16 - 18 March 2003, Hawaii Island, Hawaii*
- Richter, C. 2012, Personal communication on 28 November 2012
- SAM, 2009, *Solar Advisor Model Reference Manual for CSP Trough Systems*
- Sherry, A. 1971, *Modern power station practice volume 3: Mechanical (turbines and auxiliary equipment)*, Pergamon Press
- Singer, 1991, *Combustion fossil power*, 4<sup>th</sup> edition, Combustion Engineering Inc. Publishers

Siros, F., Philibert, C., Le Moulec, Y., Tussea, M & Bonnelle, D. 2012, The value of hybridizing CSP, *Proceedings of SolarPACES 2012, 11 – 14 September 2012, Marrakech, Morocco*

Vosoogh, A. & Hajidavalloo, 2010, Effect of variable condenser pressure, dry and wet bulb ambient temperature on the energy and exergy efficiencies of a power plant, *Proceedings of the 8th IASME /WSEAS International Conference on Fluid Mechanics & Aerodynamics (FMA '10), Heat Transfer, Thermal Engineering and Environment (HTE '10), 20 – 22 August 2010, Taipei, Taiwan*

Wagner, M.J. 2012, WREF 2012, Results and comparison from the SAM linear Fresnel technology performance model, *Proceedings of the 2012 World Renewable Energy Forum, 13 – 17 May 2012, Colorado, USA*

Wagner, M.J. & Zhu, G. 2012, A direct-steam Linear Fresnel performance model for NREL's Systems Advisor Model, *Proceedings of the ASME 2012 6<sup>th</sup> International Conference on Energy Sustainability, 23 – 26 July 2012, San Diego, USA*

Yang, Y., Yan, Q., Zhai, R., Kouzani, A. & Hu, E. 2011, An efficient way to use medium-or-low temperature solar heat for power generation – integration into conventional power plant, *Applied Thermal Engineering* 31 (2011) 157 – 162

Yan, Q., Yang, Y., Nishimura, A., Kouzani, A. & Hu, E. 2010, Multi-point and multi-level solar integration into conventional coal-fired power plant, *Energy Fuels* 2010, 24, 3733 - 3738



